

國立交通大學

光電工程研究所

碩士論文

高壓水處理技術應用於鍺型金氧半
元件之研究



**Study of High Pressure Water Treatment for
Germanium-based MOS Device**

研究生：吳明聰

指導教授：劉柏村 博士

中華民國 一 百 年 八 月

高壓水處理技術應用於鍺型金氧半元件之研究

**Study of High Pressure Water for Germanium-based MOS
Device**

研究生：吳明聰 Student：Ming-Tsung Wu

指導教授：劉柏村博士 Advisor：Dr. Po-Tsun Liu



Submitted to Department of Photonics
Institute of Electro-Optical Engineering
College of Electrical and computer Engineering
National Chiao Tung University
In partial Fulfillment of the Requirements
the Degree of
Master
In
Electro-Optical Engineering
August 2011

中華民國 一 百 年 八 月

高壓水處理技術應用於鍺型金氧半 元件之研究

研究生：吳明聰 指導教授：劉柏村 博士

國立交通大學

光電工程研究所

摘要

鍺半導體由於擁有較高的電洞和電子遷移率，被視為是下一代奈米電子元件技術中最有希望取代矽而成為電晶體主動層的半導體材料，但是次氧化鍺(GeO_x)的熱穩定性較差，使得元件製作過程中的高溫製程將會劣化Ge-MOSFET的元件特性。因此，為了消除次氧化鍺熱解造成的元件劣化情形，我們提出了高壓水處理的技術(低溫的超臨界流體)，以消除次氧化鍺熱層穩定為主要目的。所以我們研究了鍺型金氧半元件在超臨界二氧化碳流體混合水的處理下其電性的改變以及其機制探討。首先，我們對在鍺基板上剛濺鍍完的二氧化鍺使用 250°C 真空爐管退火並且做為基準片，而後再分別對其進行 300°C 、 400°C 、 500°C 通氣氣快速退火30秒，來研究其因熱所造成的元件劣化情形，接著再挑選 500°C 退火的試片對其進行溫度為 100°C 壓力為3000psi的二氧化碳超臨界流體混合水處理持續一小時；後續我們使用了高解析穿透式電子顯微鏡以及X光光電子能譜儀，驗證超臨界流體混合水能有效的使水分子擴散至二氧化鍺到達鍺通道和二氧化鍺的界面，進而再介面中產生氧化還原反應，其中包含氧化為完全鍵結的鍺元素以及還原次氧化鍺回鍺元素，使次氧化鍺層能夠消除，且整體的閘極氧化層厚度下降，也修補了因次氧化鍺熱解造成的元件劣化情形，降低閘極漏電流；對經過退火後的元件作超臨界處理，發現元件特性得到改善，顯示出超臨界二氧化碳流體混合水的確具有通過閘極氧化層進而擴散到鍺通道表面去做還原氧化的能力。除此之外，我們利用常壓的水氣快速退火來驗證是否水的處理能夠產生次氧化鍺的還原反應，由結果顯示，不論是高壓還是常壓的水處理都具有在二氧化鍺以及鍺通到界面產生氧化還原的能力，使得次氧化鍺能夠消除，不過高壓水處理的方式對於消除次氧化鍺的能力確實比常壓水處理的方式來得較具效果；通過適當的退火溫度也可以對界面產生修補的作用，所以低溫超臨界流體混合水的技術，能減少次氧化鍺層的厚度，並且改善鍺型元件的特性。可預期的，若將超臨界流體的特殊特性整合在鍺型電晶體元件的製作上，去修補因為後續高溫製程對元件產生的劣化情形，對於未來高效能鍺型MOSEFT發展，將具有其優勢以及前瞻性。

Study of High Pressure Water Treatment for Germanium-based MOS Device

Student : Ming-Tsung Wu

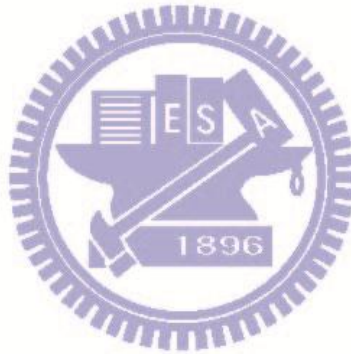
Advisor : Dr. Po-Tsun Liu

Department of Photonics Institute of Electro-Optical Engineering
National Chiao Tung University

Abstract

Germanium (Ge) semiconductor has been considered as an alternative channel material in replace of Si for future high-performance CMOS technology, because its higher carrier mobility for both electrons (2.6 times) and holes (4.2 times). However, the Ge-MOS technology has the most critical issue hindering the application of Ge is lack of high-quality and stable Ge sub-oxide (GeO_x). In this study, to solve the thermal decomposition of GeO_x the high pressure water treatment (supercritical fluids technology) is employed originally to eliminate the GeO_x interlayer and improve the properties of ZrO_2 high-k film. First, the thermal stability of ZrO_2/Ge stack is analyzed by the sample treated with 250°C high vacuum furnace annealing for 30min and then treated by 300°C , 400°C and 500°C N_2 RTA for 30s respectively. Second, the high pressure water treatment (SCF) at 100°C and 3000psi for 1hr used to the sample which is treated by 500°C N_2 RTA for 30s. By HR-TEM, XPS analyses, it can verify

the elimination of GeO_x interlayer due to the SCF treatment surely, and it can explain the improvement of the gate leakage after SCF treatment. According to the many reference paper, we indicate the mechanism about the reduction of GeO_x interlayer in ZrO_2/Ge by SCF treatment. Besides, the Water Vapor Annealing is used to verify the water treatment has the ability of redox in the ZrO_2/Ge stack, and though the annealing by suitable temperature can repair the interface to improve the electric characteristic of ZrO_2/Ge device. The SCF treatment on high performance Ge-MOSFET shows promise as critical technology in resolving GeO_x decomposition.



誌 謝

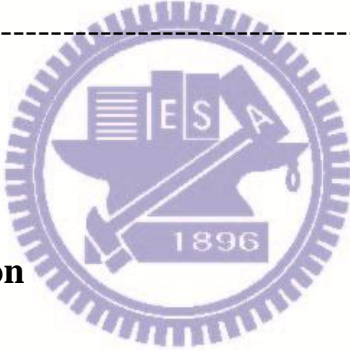
首先我要先感謝我的指導教授：劉柏村教授，提供完好的研究環境以及豐富的資源，並且在實驗上給予我寶貴的意見讓我受益良多。除了有完善的設備、高水準的師資與研究團隊可以隨時與世界頂尖研究成果爭雄，實驗室注重文能力培養也讓我不忘踏出自己關門的研究，培養國際化的能力與視野，成為全方位的人才，未來可以為校爭光回饋社會。

在這兩年來研究的旅途上，我最感謝指導我的學長黃震鑠學長，常常不厭其煩的教導我如何研究、如何安排與規劃實驗，也教導我許許多多在學術上我遇到挫折該如何去面對，真的是由衷的感激；再來感謝其他實驗室的學長，鄒一德、鄧立峯和竹立煒學長，時時不斷的給我關心以及共度生活上的一些瑣事；也感謝陪伴我的實驗室的同學楊孟娟與范揚順，一起研究一起休閒，有了他們讓實驗生活更加多采多姿；此外，還要感謝學弟妹們，不論是在實驗上還是實驗室生活的陪伴，有你們真好。

最後，也是最重要的，要感謝我的父母吳塗情先生以及黃玉清小姐，感謝他們的養育之恩，常常在我最困頓的時候給予我莫大的鼓勵與支持，千言萬語都說不來我對父母的愛與感謝；另外，特別要感恩我生命中的導師，您給予我的，我只能用全力以赴的心，以報師恩；感謝大家的支持與陪伴，讓我可以順利的邁向人生的下一階段，感謝有你們。

吳明聰 2011 年 8 月

Contents

Chinese Abstract	-----	i
English Abstract	-----	iii
Chinese Acknowledgment	-----	v
Contents	-----	vi
Table Captions	-----	ix
Figure Captions	-----	x
		
Chapter 1 Introduction		
1.1 General Background	-----	1
1.2 Motivation	-----	4
1.3 Organization of Thesis	-----	6
Chapter 2 Experiment Instrument and Process		
2.1 Experiment Instruments	-----	10
2.1.1 RF - Sputter	-----	10
2.1.2 Water Vapor Rapid Thermal Annealing System	-----	12
2.1.3 Supercritical Fluid System	-----	14

2.2 Process Flow of Zirconium Oxide on Germanium Substrate	
Metal-Insulator-Semiconductor Capacitor Fabrication -----	18
2.3 Analysis Methods -----	22
2.3.1 Methods of Electrical Characteristics -----	22
2.3.1.1 Parameters Extraction -----	22
2.3.2 Methods of Material analysis -----	23
2.3.2.1 X-ray Photoelectron Spectroscopy -----	23
2.3.2.2 High-Resolution Transmission Electron Microscopy -----	25

Chapter 3 Results and Discussion

3.1 Effect of Supercritical Fluid and Post-Deposition Annealing on the ZrO ₂ /Ge MOS-Capacitor -----	26
3.1.1 Thermal Stability of ZrO ₂ /Ge MOS-Capacitor -----	26
3.1.2 Effect of Supercritical Fluid Treatment -----	31
3.2 Effect of Water Vapor Annealing on the ZrO ₂ /Ge MOS- Capacitor -----	41
3.2.1 Compare with Water Vapor Annealing and Nitrogen Annealing -----	41
3.2.2 Combination of Supercritical Fluid and Water Vapor Annealing -----	50
3.3 Summaries -----	51

Chapter 4 Conclusions and Future Works

4.1 Conclusions ----- 53

4.2 Future works ----- 54

Reference ----- 55

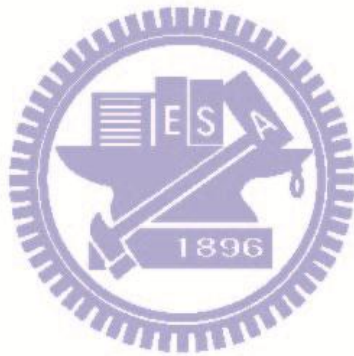


Table Captions

Chapter 1

Table 1-1 Critical temperature and pressure for some common fluids. ----- 9

Chapter 2

Table 2-1 Comparison of physical properties of CO₂. ----- 17

Chapter 3

Table 3-1 The parameter of C-V characteristics for ZrO₂/Ge with various thermal treatments. ----- 31

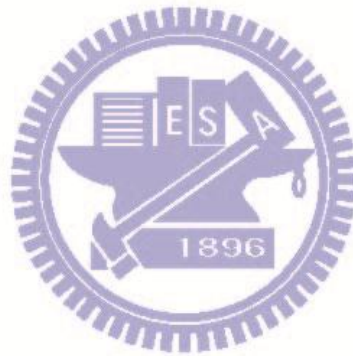


Figure Captions

Chapter 1

Fig. 1-1 Phase diagram for CO₂. ----- 9

Chapter 2

Fig. 2-1 RF sputtering. ----- 11

Fig. 2-2 Rapid thermal annealing system. ----- 13

Fig. 2-3 Water vapor system. ----- 13

Fig. 2-4 The supercritical fluid element. ----- 15

Fig. 2-5 Density-pressure-temperature surface for pure CO₂. ----- 16

Fig. 2-6 The supercritical fluid system. ----- 16

Fig. 2-7 Schematic of cleaning high aspect ratio structures with liquids and supercritical fluids. ----- 17

Fig. 2-8 The experiment flows of ZrO₂/Ge capacitor with different PDA treatment and SCF treatment. ----- 21

Fig. 2-9 The experiment flows of ZrO₂/Ge capacitor with wet N₂ treatment. ----- 21

Chapter 3

Fig. 3-1 The gate leakage current density of sputtered-ZrO₂ on Ge with various thermal treatments. ----- 29

Fig. 3-2 The gate leakage current density of sputtered-ZrO₂ on Si with various thermal treatments. ----- 29

Fig. 3-3 The C-V characteristics of ZrO₂/Ge with various thermal treatments. ---- 30

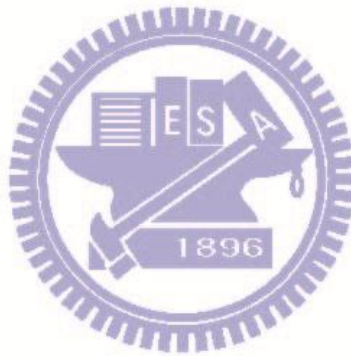
Fig. 3-4	The gate leakage current density of 500°C RTA-treated condition on Ge with and w/o SCF treatment. -----	34
Fig. 3-5	The cross-sectional HRTEM images of sputtered-ZrO ₂ on Ge with high vacuum annealing at 250 °C (a) w/o and (b) with RTA treatment at 500 °C. -----	35
Fig. 3-6	The cross-sectional HRTEM images of sputtered-ZrO ₂ on Ge with high vacuum annealing at 250 °C and 500 °C RTA (a) w/o and (b) with SCF treatment. -----	35
Fig. 3-7	The XPS spectra of Ge 2 <i>p</i> _{3/2} with various treatments. -----	36
Fig. 3-8	The XPS spectra of Zr 3 <i>p</i> _{3/2} with various treatments. -----	36
Fig. 3-9	The transporting mechanism for SCCO ₂ fluids taking H ₂ O molecule into dielectric film. -----	37
Fig. 3-10	The schematic diagram of GeO _x reduction reactions on the interfacial layer. -----	37
Fig. 3-11	Depth profiles of Zr, O and Ge atoms in ZrO ₂ /Ge after high vacuum annealing at 250 °C for 30 min by XPS. -----	38
Fig. 3-12	Depth profiles of Zr, O and Ge atoms in ZrO ₂ /Ge after high vacuum annealing at 250 °C for 30min and 250 °C RTA for 30sec by XPS. -----	39
Fig. 3-13	Depth profiles of Zr, O and Ge atoms in ZrO ₂ /Ge after high vacuum annealing at 250 °C for 30 min, 250 °C RTA for 30sec and SCF for 60min by XPS. -----	40
Fig. 3-14	The gate leakage current density of ZrO ₂ /Ge with 300°C H ₂ O and N ₂ RTA. -----	45
Fig. 3-15	The C-V characteristics of ZrO ₂ /Ge with 300°C H ₂ O and N ₂ RTA. -----	45
Fig. 3-16	The XPS spectra of Ge 2 <i>p</i> _{3/2} with 300°C H ₂ O and N ₂ RTA. -----	46
Fig. 3-17	The XPS spectra of Ze 3 <i>p</i> _{3/2} with 300°C H ₂ O and N ₂ RTA. -----	46

Fig. 3-18 Depth profiles of Zr, O and Ge atoms in ZrO₂/Ge with STD condition by XPS. ----- 47

Fig. 3-19 Depth profiles of Zr, O and Ge atoms in ZrO₂/Ge with Water Vapor Annealing at 300 °C for 3 min by XPS. ----- 48

Fig. 3-20 Depth profiles of Zr, O and Ge atoms in ZrO₂/Ge with Dry Nitrogen Annealing at 300 °C for 3 min by XPS. ----- 49

Fig. 3-21 The C-V characteristics of ZrO₂/Ge with combining SCF and 300°C H₂O RTA. ----- 51



Chapter 1

Introduction

1.1 General Background

From the 1960s to current IC industry, Moore's Law is the key to lead the semiconductor industry; it's say that the number of transistors per unit area has doubled every 18 months. That means more transistors are integrated on a chip, enabling higher performance and reduced cost. To follow Moore's Law, the dimension of transistors must continue to be scaling down. However, as the channel length and gate oxide thickness of complementary metal oxide semiconductor (CMOS) devices continuous to shrink, short-channel effect ^[1] and power consumption ^[2] are critical problems we faced separately.

For the metal-oxide-semiconductor field-effect transistor (MOSFET), the drive current can be representation of the performance of MOSFET device, higher drive current indicate higher performance. The first order current-voltage approximation drive current in saturation region is expressed as

$$I_{DS} = \frac{1}{2} \frac{W}{L} \mu C_{OX} (V_{GS} - V_T)^2 \quad (1-1)$$

$$C_{OX} = \frac{\epsilon_{OX}}{t_{OX}} \quad (1-2)$$

Where W is the channel width, L is the effective channel length, μ is the mobility of channel material, C_{OX} is the gate oxide capacitance per unit area, V_{GS} is the voltage applied on gate to source, V_T is the threshold voltage, ϵ_{OX} is the dielectric constant of gate oxide, t_{OX} is the gate oxide thickness. As feature size is scale down, gate length (L) and oxide thickness (t_{OX}) shrink to lead high drive current, as scale down continuously, the above mention problems become the dramatic challenges because physical limitation of size effect. Elevating channel mobility is a way to get higher performance and avoid size issues. Enable to get high mobility for silicon based CMOS, there are two major technology; vertical structure ^[3,6] and channel strain [4,5] can enhance mobility of silicon channel about dozens percent ^[4,5]. Although the techniques can improve carrier mobility to get high performance of silicon based CMOS devices, but also face to the problems of processing is too complicated, low throughput and poor yield make cost too high. To resolve the challenges and still keep CMOS performance ongoing, a simple and intuitive way is replace silicon with new channel material.

Germanium (Ge) semiconductor has been considered as a alternative channel material in replace of Si for future high-performance CMOS technology, because its higher carrier mobility for both electrons (2.6 times) and holes (4.2 times), lower dopant thermal activation energies for shallower junction formation and compatible

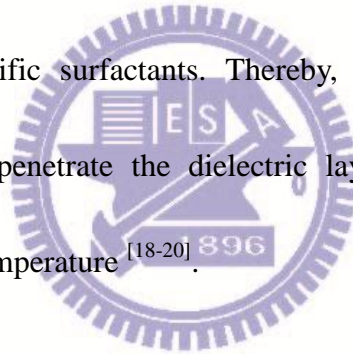
fabrication processes with existing silicon manufacturing infrastructure. However, the Ge-MOS technology still has many challenges and not been widely deployed. The most critical issue hindering the application of Ge is lack of high-quality and stable Ge insulation oxide comparable to silicon dioxide (SiO₂) for silicon [7, 8]. The poor native Ge oxide (GeO₂) layer would be soluble in water and thermally decomposed at low temperature (about 420°C) induced Ge diffuses into gate dielectric layer during the thermal deposition or post-deposition annealing (PDA) processes. The reaction of GeO₂ decomposition can be expressed as



Sequentially, poor interface properties and high gate leakage current will be exhibited in the Ge-MOS device [9-13]. Various pre-gate surface modification techniques, such as surface nitridation or Si passivation, have been developed to improve the quality of gate insulator/Ge interface [14]. It was also reported that high-performance Ge MOSFET could be realized by careful control of interfacial GeO₂ formation [8]. In my thesis, first, a low-temperature supercritical CO₂ (SCCO₂) fluid technology is proposed as a post-gate dielectric treatment at 100°C to reduction the Ge-suboxide in dielectric/Ge interface after high-temperature PDA process. On the second hand, the low temperature water vapor RTA with N₂ to reduce the defect on the interface after reduction of Ge-suboxide. In summary, we can form the Ge

MOS-C with low gate leakage and good interface of Ge with dielectric.

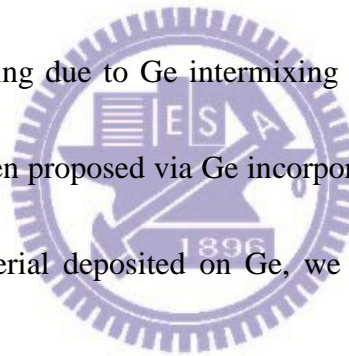
The supercritical fluid (SCF), which exists above specific critical pressure and temperature, as shown in Fig 1-1 ^[15, 16]. It provides good liquid-like solvency and high gas-like diffusivity, giving it excellent transport capacity ^[17]. Table 1-1 shows critical pressure and temperature for some common fluids. CO₂ is easy to acquire and safe to be as supercritical fluid and it is easy to achieve supercritical state, low critical temperature (room temperature at 30°C) and not high critical pressure (1072psi = 72.8 atm), non-toxic, non-flammable, and inexpensive. The oxidant is also easily dissolved in SCCO₂ fluid with specific surfactants. Thereby, we choose SCCO₂ fluid to transport the oxidant and penetrate the dielectric layer for trap passivation and interface oxidation at low temperature ^[18-20].



1.2 Motivation

To achieve a low temperature process on Ge-MOS device, high-k material is a good candidate to be gate dielectric for Germanium substrate. There are at least four requirements to form gate dielectric on Germanium. First, the dielectric constant must be high (>20). Second, must be thermodynamic stable with Ge, the high-k material does not react with the Ge during depositing, to avoid a low-k interfacial layer formed during depositing, and make the dielectric constant of high-k material decrease. Third,

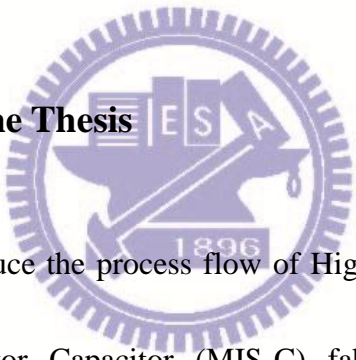
large enough band offset with Ge ($>1\text{eV}$), enough barrier high between Ge and gate dielectric can prevent the high leakage by carriers get thermal energy to overcome the barrier between Ge and gate oxide and to create leakage. Forth, form a good interface with Ge. The hafnium oxide (HfO_2) and the zirconium oxide (ZrO_2) are meeting the above four conditions, and have been widely studied. For high-k metal gate, HfO_2 is widely used in 45nm processing. Because of it has better thermodynamic stability than ZrO_2 on silicon. However, for germanium as the channel material, ZrO_2 is more compatible than HfO_2 , because of less interfacial layer which is low-k layer formed after post-deposition annealing due to Ge intermixing in ZrO_2 ^[21]. In addition, very high-k ($k\sim 37$) ZrO_2 have been proposed via Ge incorporation into ZrO_2 ^[22]. Therefore, ZrO_2 is a good high-k material deposited on Ge, we choose ZrO_2 as our research high-k material.



Among several metal oxide films formations, in general, low temperature deposition is prefer, because of the low thermal budget and low costs. However, the low-temperature deposition films may cause poor interfacial properties with substrate and larger leakage current due to numerous traps inside the bulk metal oxide film. Proper annealing can reduced leakage and remove oxide charges and interface traps in the ZrO_2 . But for germanium substrate, the thermal stability of GeO_2 is a critical problem to form a good Ge-MOS. Because PDA or following high-temperature

processes (like S/D annealing) could induce Ge decomposition into gate dielectric and increase leakage source enhance the leakage current after annealing. On my thesis, we use the low-temperature (100°C) technique supercritical fluid (SCF) to transport the oxidant and penetrate the dielectric layer for trap passivation and interface oxidation at low temperature. And by leakage current fitting to see how leakage mechanism transfers after SCF treats. Next, to repair the interface of ZrO_2/Ge after SCF treatment we use the Water Vapor Annealing. And then we combine these methods to form a good interface of ZrO_2/Ge .

1.3 Organization of the Thesis



In chapter 2, we introduce the process flow of High-k on Germanium substrate Metal-Insulator-Semiconductor Capacitor (MIS-C) fabrication first. Second, the process instruments are introduced about RF-sputter, Vacuum Annealing Furnace, Rapid Thermal Annealing, Supercritical Fluid (SCF), Thermal coater. Third, electrical characteristics analysis instrument and material characteristics analysis instrument about X-ray Photoelectron Spectroscopy (XPS) and High-Resolution Transmission Electron Microscopy (HRTEM) are all introduced. Finally, the parameters extraction and transportation mechanism are also discussed in this chapter.

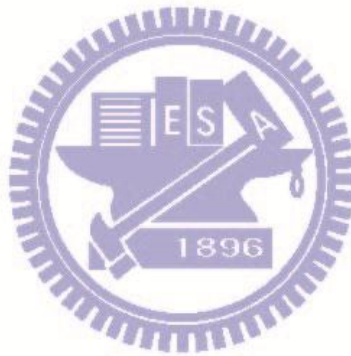
In chapter 3, there are two parts, we first study the effect of two steps PDA on

the ZrO_2 film which deposited by sputter on Germanium substrate, then discussing the thermal stability and the quality of high-k film. Then we accede Supercritical Fluid treatment(SCF) to our work and analyze in various electrical analysis techniques, such as capacitance-voltage (CV) and current density-voltage (JV) by Agilent 4980 and Keithley 4200 were perform to characteristic the device performance and analysis the interface and bulk quality of gate dielectric. For material analysis, such as x-ray photoelectron spectroscopy (XPS) and high-resolution transmission electron microscopy (HRTEM) to analyze variation of the interface after PDA and SCF.

On the second part, this section is continued from the preceding paragraph. First, we deposit the ZrO_2 high-k gate dielectric on Ge substrates, and then anneal by using rapid thermal annealing with wet nitrogen (with water vapor). The annealing in water vapor can suppress growth of unstable low-k GeO_x interlayer in Ge metal-oxide-semiconductor capacitor with high-k gate dielectric ^[23] by reducing the GeO_x to Ge and through the low thermal budget process can repair the defect which produced by reduction of GeO_x in the interlayer. Second, to compare annealing with and without water, we use the rapid thermal annealing with nitrogen to compare with water vapor annealing. By analyzing C-V and J-V curve which help us to understand the recovery of the defect in interlayer after GeO_x reduction whether it need oxygen or not. And various material analysis techniques, such as high-resolution transmission

electron microscopy (HRTEM), x-ray photoelectron spectroscopy (XPS), were performed to characteristic the cross section of device and surface morphology. In the end, we combine the Supercritical Fluid treatment and water vapor annealing to form the device with good interface and low defect in the bulk high-k dielectric.

Finally, in chapter 4, we give the conclusions and suggestions of the thesis for the future work.



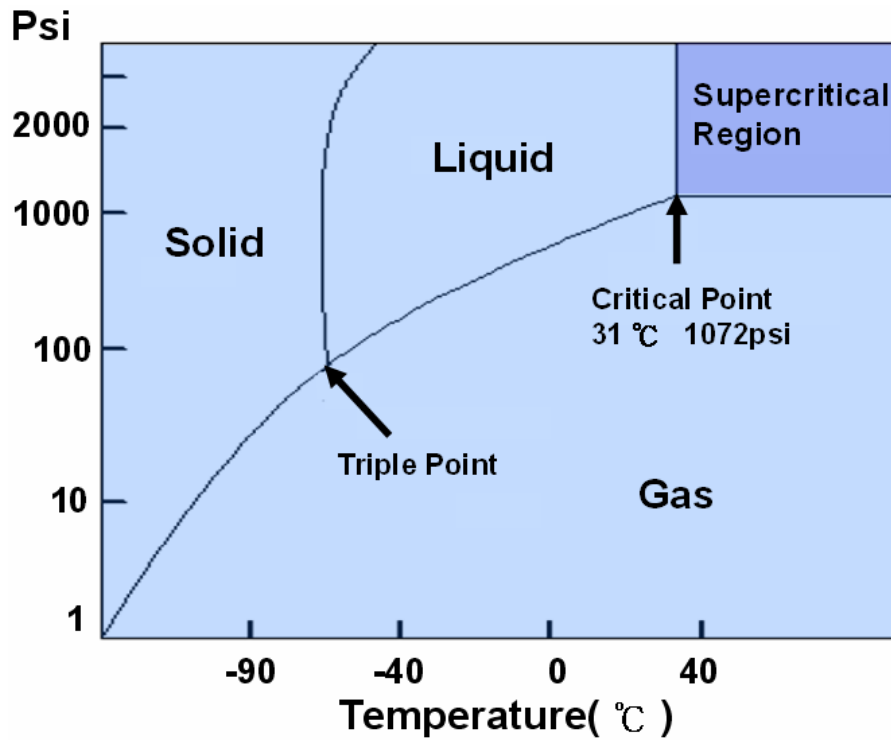


Fig. 1-1 Phase diagram for CO₂.

Fluid	Critical Temperature(°C)	Critical Pressure (Psi) (1atm=14.7psi)
Helium (He)	-268	33
Neon (Ne)	-229	400
Argon (Ar)	-122	706
Nitrogen (N ₂)	-147	492
Oxygen (O ₂)	-119	731
Carbon dioxide (CO ₂)	31	1072
Sulfur hexafluoride (SF ₆)	46	545
Ammonia (NH ₃)	133	1654
Water (H ₂ O)	374	3209

Table 1-1 Critical temperature and pressure for some common fluids.

Chapter 2

Experiment Instrument and Process

2.1 Experiment instrument of High-k on Germanium base Metal-Insulator-Semiconductor Capacitor

2.1.1 RF Sputtering

Sputter deposition is a physical vapor deposition (PVD) method of depositing thin films by sputtering, that is ejecting, material from a "target," that is source, which then deposits onto a "substrate," such as a silicon wafer. Resputtering is re-emission of the deposited material during the deposition process by ion or atom bombardment. Sputtered atoms ejected from the target have a wide energy distribution, typically up to tens of eV (100,000 K). The sputtered ions (typically only a small fraction — order 1% — of the ejected particles are ionized) can ballistically fly from the target in straight lines and impact energetically on the substrates or vacuum chamber (causing resputtering). Alternatively, at higher gas pressures, the ions collide with the gas atoms that act as a moderator and move diffusively, reaching the substrates or vacuum chamber wall and condensing after undergoing a random walk. The entire range from high-energy ballistic impact to low-energy thermalized motion is accessible by changing the background gas pressure. The sputtering gas is often an inert gas such as argon. For efficient momentum transfer, the atomic weight

of the sputtering gas should be close to the atomic weight of the target, so for sputtering light elements neon is preferable, while for heavy elements krypton or xenon are used. Reactive gases can also be used to sputter compounds. The compound can be formed on the target surface, in-flight or on the substrate depending on the process parameters. The availability of many parameters that control sputter deposition make it a complex process, but also allow experts a large degree of control over the growth and microstructure of the film. Charge build-up on insulating targets can be avoided with the use of RF sputtering where the sign of the anode-cathode bias is varied at a high rate, as Fig. 2-1. RF sputtering works well to produce highly insulating oxide films but only with the added expense of RF power supplies and impedance matching networks. Stray magnetic fields leaking from ferromagnetic targets also disturb the sputtering process. Specially designed sputter guns with unusually strong permanent magnets must often be used in compensation.

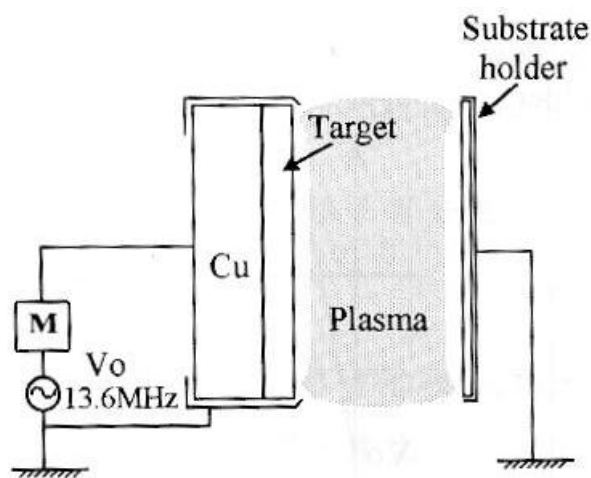


Fig. 2-1 RF sputtering.

2.1.2 Water Vapor Rapid Thermal Annealing System

Rapid Thermal Anneal (RTA) is a subset of Rapid Thermal Processing as Fig. 2-2. It is a process used in semiconductor device fabrication which consists of heating a single wafer at a time in order to affect its electrical properties. Unique heat treatments are designed for different effects. Wafers can be heated in order to activate dopants, change film-to-film or film-to-wafer substrate interfaces, density deposited films, change states of depositing films, repair damage from ion implantation, move dopants or drive dopants from one film into another or from a film into the wafer substrate. Rapid thermal anneals are performed by equipment that heats a single wafer at a time using either lamp based heating, a hot chuck, or a hot plate that a wafer is brought near. Unlike furnace anneals they are short in duration, processing each wafer in several minutes. To achieve short time annealing time trade off is made in temperature and process uniformity, temperature measurement and control and wafer stress as well as throughput. And it can change the input gas to achieve different thermal treatment, even water vapor system, Fig. 2-3. Recently, RTP-like processing has found applications in another rapidly growing field — solar cell fabrication. RTP-like processing, in which an increase in the temperature of the semiconductor sample is produced by the absorption of the optical flux, is now used for a host of solar cell fabrication steps, including phosphorus diffusion for N/P junction formation

and impurity gettering, hydrogen diffusion for impurity and defect passivation, and formation of screen-printed contacts using Ag-ink for the front and Al-ink for back contacts, respectively.

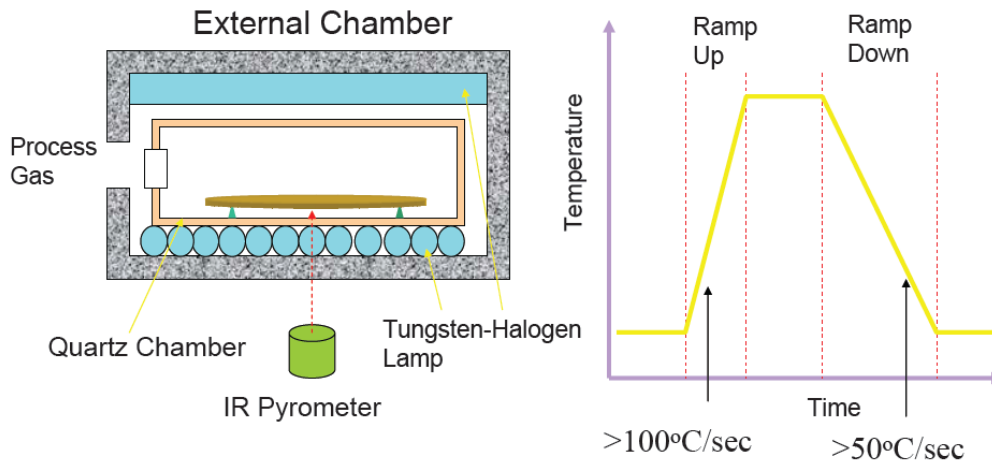


Fig. 2-2 Rapid thermal annealing system.

Bubbler

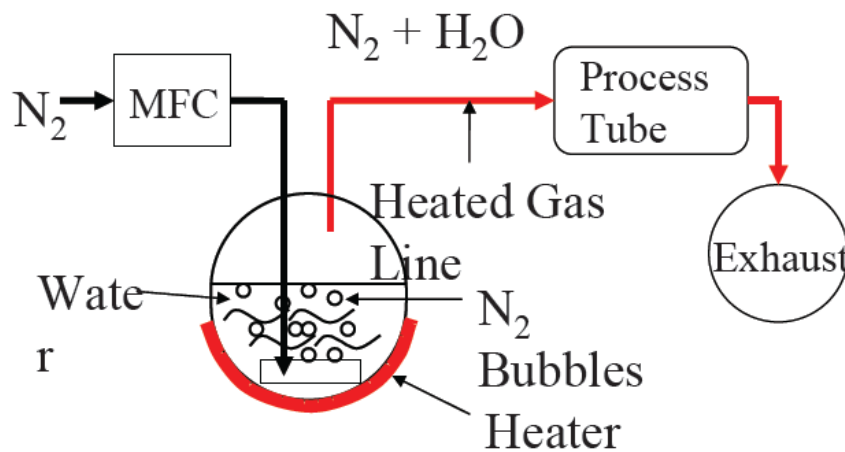


Fig. 2-3 Water vapor system.

2.1.3 Supercritical Fluid System

Supercritical fluid (SCF) is compound above their critical temperatures and pressure, as shown in Fig 1-1. ^[15, 16] The attractiveness of supercritical fluid for commercial applications is their unique combination of liquid-like and gas-like properties. The supercriticality is a strange and intriguing state in which solids can dissolve in gases, and liquids can alternate between reflectivity and transparency. The critical temperature and pressure for some common supercritical fluids are displayed in Table 1-1. The CO₂-based supercritical fluid is particularly attractive because CO₂ is non-toxic, non-flammable, recyclable, and inexpensive and has a reasonably high solvent power for most organic components. Besides, its critical conditions are easily achievable with existing process equipment (31 °C, 1072 psi =72.8 atm).

Figure 2-5 shows the density-pressure-temperature surface for pure CO₂. It can be discovered that relatively small changes in temperature or pressure near the critical point, resulting in large changes in density. Table 2-1 shows the comparison of several physical properties of typical liquid, vapor, and supercritical fluid state for CO₂. It could be seen that supercritical CO₂ (SCCO₂) fluid possesses liquid-like density, so that SCCO₂ fluid is analogous with light hydrocarbon to dissolve most solutes and own exceptional transport capability. ^[24, 25] On the other hand, SCCO₂ fluid hold

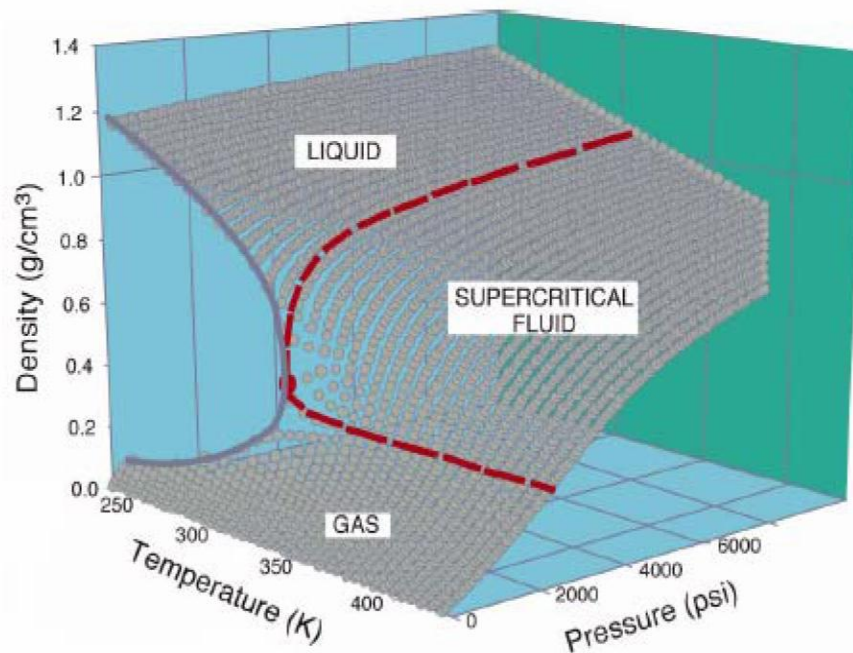


Fig. 2-5 Density-pressure-temperature surface for pure CO₂.^[25]

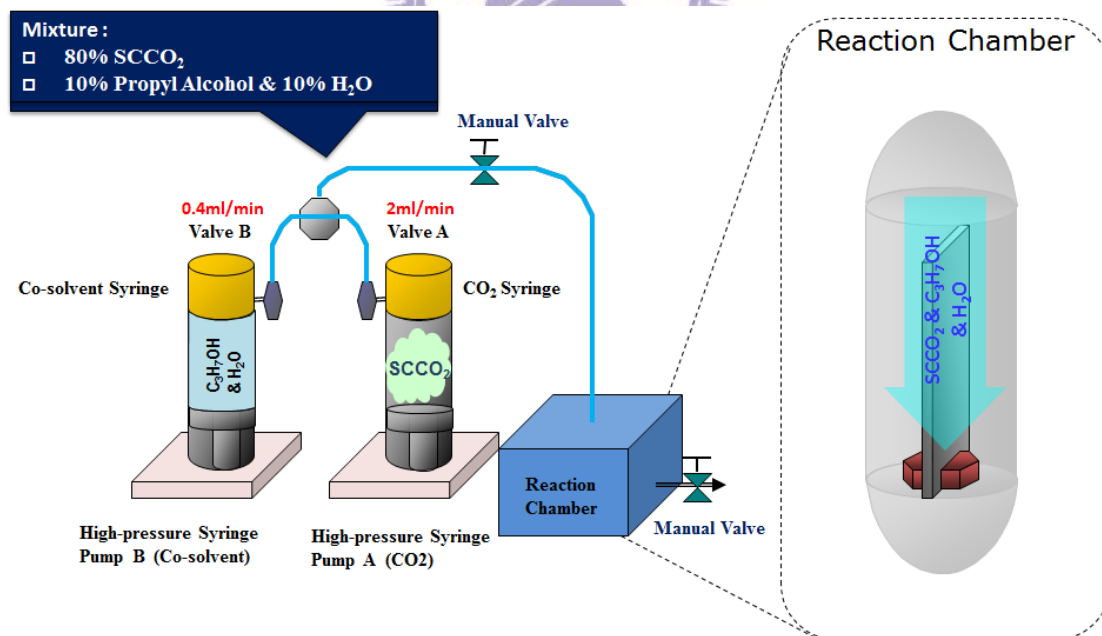


Fig. 2-6 The supercritical fluid system.

	Liquid	Supercritical Fluid	Vapor
Density (g/cm ³)	1.0	0.3 ~ 0.7	~ 10 ⁻³
Diffusivity (cm ² /sec)	< 10 ⁻⁵	10 ⁻² ~ 10 ⁻⁵	~ 10 ⁻¹
Viscosity (g/cm-sec)	~ 10 ⁻²	10 ⁻³ ~ 10 ⁻⁶	~ 10 ⁻⁶

Tab. 2-1 Comparison of physical properties of CO₂.^[26]

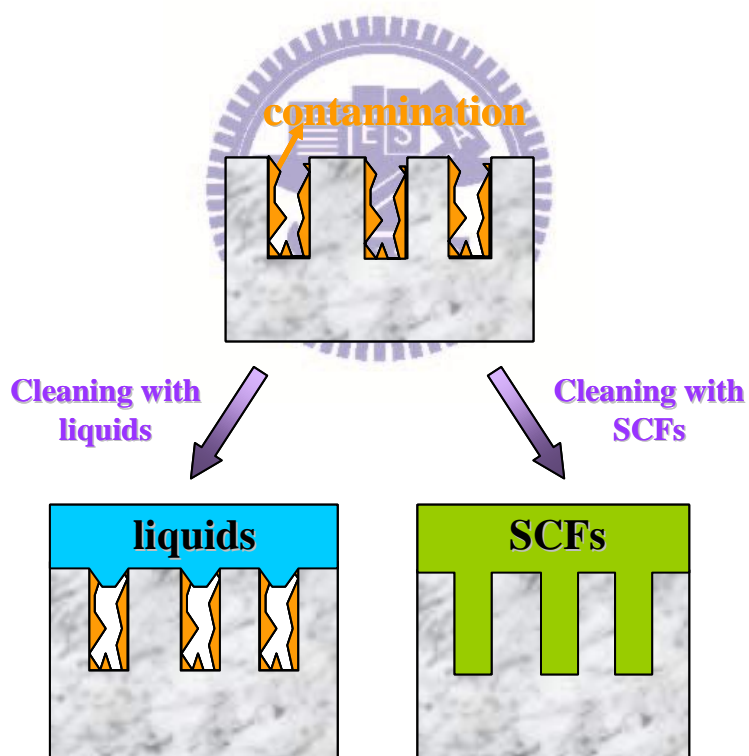


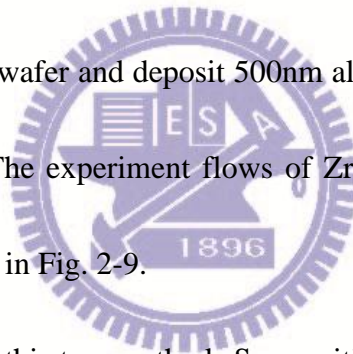
Fig. 2-7 Schematic of cleaning high aspect ratio structures with liquids and supercritical fluids.

2.2 Process Flow of Zirconium Oxide on Germanium Substrate Metal-Insulator-Semiconductor Capacitor (MIS-C) Fabrication

A 0.003 ohm-cm p-type (100) Ge wafer was cleaned with cycling DHF clean process and immediately loaded into the sputter chamber. As the chamber pressure reached to the 2×10^{-6} torr, about 5nm ZrO₂ film was deposited by RF-sputter. First, the sample was subjected to the post deposition annealing, first under 250°C for 30min in high vacuum furnace to be the STD sample, and then anneal with 300°C, 400°C and 500°C for 30sec by rapid temperature annealing (RTA) in nitrogen environment, separately. The SCF treatment was performed right after the 500°C RTA to repair the device performance. The sample was placed in a SCF system at 100°C for 1 hr, where was injected with 3000 psi of SCCO₂ fluid that were mixed with 10 vol.% of propyl-alcohol and 10 vol.% of DI water. Finally, deposit 100nm tantalum-nitride electrodes by sputter and 500nm aluminum electrodes by thermal evaporation on the top surface of ZrO₂ film with two electrode areas of 3.14×10^{-4} cm² and 2.83×10^{-3} cm², then BOE the back side of germanium wafer and deposit 500nm aluminum as back electrodes to fabricate MOS capacitors. The experiment flows of ZrO₂/Ge capacitor with various treatments are exhibited in Fig. 2-8.

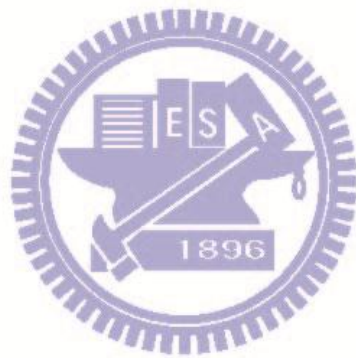
Second, a 0.003 ohm-cm p-type (100) Ge wafer was also cleaned with cycling

DHF clean process and immediately loaded into the sputter chamber. As the chamber pressure reached to the 2×10^{-6} torr, about 5nm ZrO₂ film was deposited by RF-sputter. There are two environment for rapid thermal annealing, first, the sample was annealed by using rapid thermal annealing in wet nitrogen (with water vapor) environment with 300°C for 3mins. Another is annealing in dry nitrogen environment without oxygen with 300°C for 3mins. Finally, deposit 100nm tantalum-nitride electrodes by sputter and 500nm aluminum electrodes by thermal evaporation on the top surface of ZrO₂ film with two electrode areas of 3.14×10^{-4} cm² and 2.83×10^{-3} cm², then use BOE to the back side of germanium wafer and deposit 500nm aluminum as back electrodes to fabricate MOS capacitors. The experiment flows of ZrO₂/Ge capacitor with various treatments are also exhibited in Fig. 2-9.



In the end, we combine this two methods Supercritical Fluid treatment and water vapor annealing to form the device with good interface and low defect in the bulk high-k dielectric. First, we deposit about 5nm ZrO₂ film on Ge substrate by RF-sputter, and then anneal with 500°C for 30sec by Rapid Temperature Annealing (RTA) in nitrogen environment. Second, we use the Supercritical Fluid treatment (SCF) with 100°C and 3000psi for 1hr, and then anneal with 300°C for 3min by Rapid Temperature Annealing (RTA) in wet nitrogen environment (water vapor and nitrogen). The last, we deposit 100nm tantalum-nitride electrodes by sputter and

500nm aluminum electrodes by thermal evaporation on the top surface of ZrO_2 film and bottom of substrate.



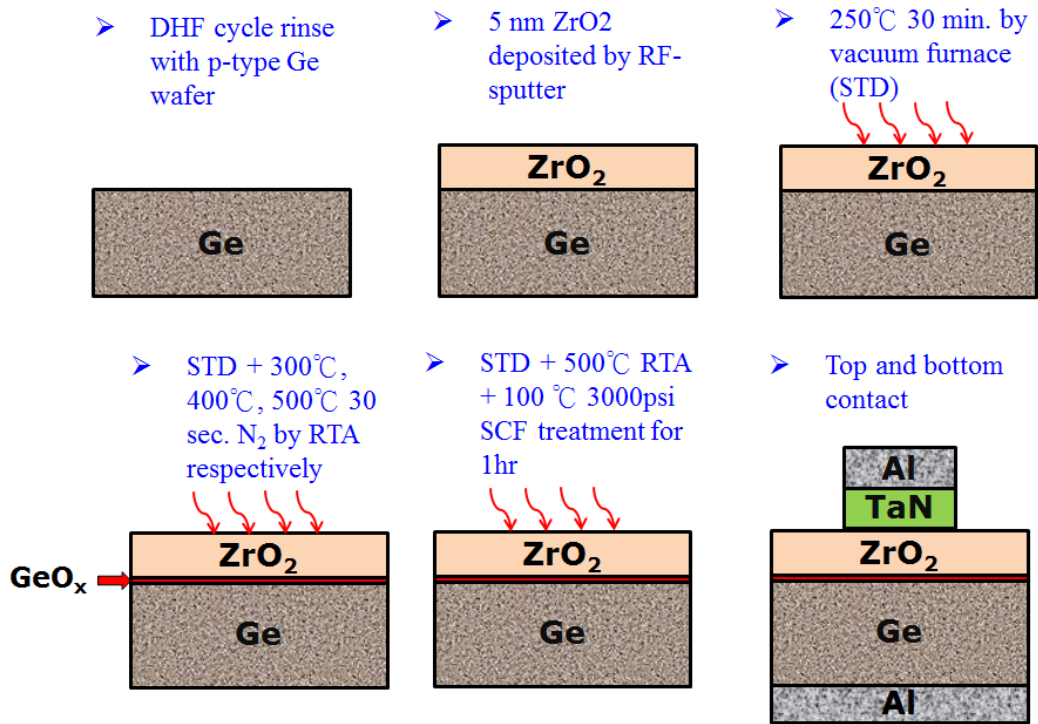


Fig. 2-8 The experiment flows of ZrO₂/Ge capacitor with different PDA treatment and SCF treatment.

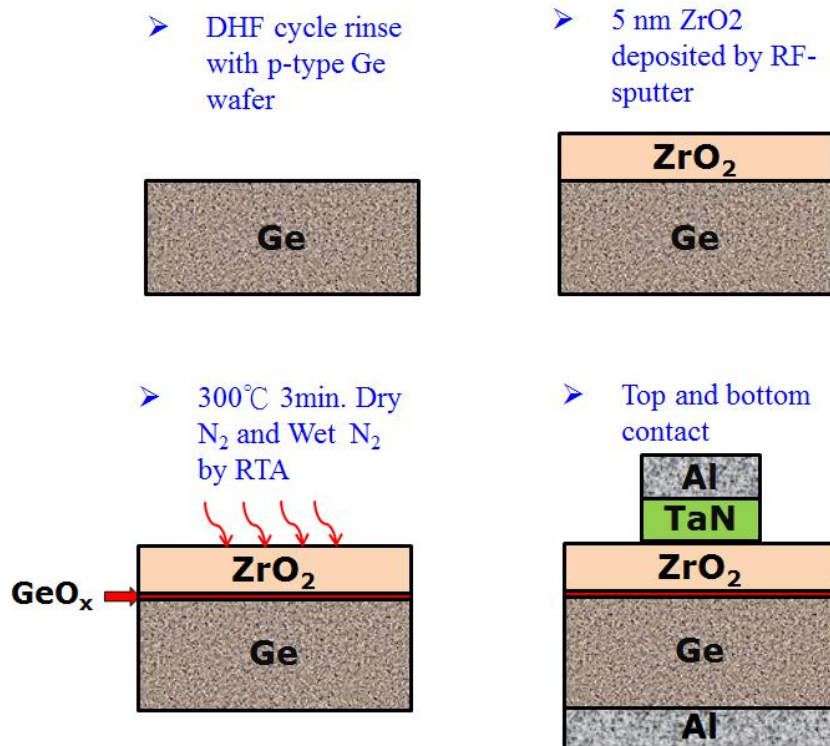


Fig. 2-9 The experiment flows of ZrO₂/Ge capacitor with wet N₂ treatment.

2.3 Analysis Methods

2.3.1 Methods of Electrical Characteristics

2.3.1.1 Parameter Description

There are three parameters represent the characteristics of MOS capacitors.

➤ **Effective Oxide Thickness (EOT)**

$$C_{ox} = \frac{\epsilon_{SiO_2} A}{EOT} = \frac{\epsilon_{ZrO_2} A}{d_{thick.}} \quad (2-1)$$

$$EOT = \frac{\epsilon_{SiO_2}}{\epsilon_{ZrO_2}} d_{thick.} \quad (2-2)$$

Eq. (2-1) represents the gate oxide capacitance equivalent thickness of the SiO₂, Eq. (2-2) represents the effective oxide thickness (EOT) related to the dielectric constant of ZrO₂. For the Eq. (2-2), the less EOT represents the value of k is higher.

Where ϵ_{SiO_2} is dielectric constant of SiO₂, ϵ_{ZrO_2} is dielectric constant of ZrO₂, d_{thick} is thickness of ZrO₂.

➤ **Flat Band Voltage (V_{fb})**

$$V_{FB} = \phi_{ms} - \frac{Q_o}{C_{ox}} \quad (2-3)$$

Eq. (2-3) represents the number of charge exists inside the dielectric, that means the V_{fb} near the zero bias, the less oxide charges existing inside the dielectric. Where

ϕ_{ms} is the work function difference between gate and substrate, Q_0 is the number of oxide charges in the dielectric.

➤ **Hysteresis (ΔV_{fb})**

Hysteresis represents the quality of interface between the dielectric and substrate, smaller ΔV_{fb} indicate better interface quality.

2.3.2 Methods of Material analysis

2.3.2.1 X-ray Photoelectron Spectroscopy

X-ray photoelectron spectroscopy (XPS) is a quantitative spectroscopic technique that measures the elemental composition, empirical formula, chemical state and electronic state of the elements that exist within a material. XPS spectra are obtained by irradiating a material with a beam of X-rays while simultaneously measuring the kinetic energy and number of electrons that escape from the top 1 to 10 nm of the material being analyzed. XPS requires ultra high vacuum (UHV) conditions. XPS is a surface chemical analysis technique that can be used to analyze the surface chemistry of a material in its "as received" state, or after some treatment, for example: fracturing, cutting or scraping in air or UHV to expose the bulk chemistry, ion beam etching to clean off some of the surface contamination, exposure

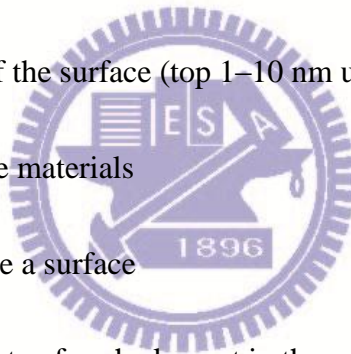
to heat to study the changes due to heating, exposure to reactive gases or solutions, exposure to ion beam implant, exposure to ultraviolet light.

➤ XPS is also known as **ESCA**, an abbreviation for **Electron Spectroscopy for Chemical Analysis**.

➤ XPS detects all elements with an atomic number (Z) of 3 (lithium) and above. It cannot detect hydrogen ($Z = 1$) or helium ($Z = 2$) because the diameter of these orbital is so small, reducing the catch probability to almost zero.

XPS is used to measure:

- elemental composition of the surface (top 1–10 nm usually)
- empirical formula of pure materials
- elements that contaminate a surface
- chemical or electronic state of each element in the surface
- uniformity of elemental composition across the top surface (or line profiling or mapping)
- uniformity of elemental composition as a function of ion beam etching (or depth profiling)



2.3.2.2 High-Resolution Transmission Electron Microscopy

High-resolution transmission electron microscopy (HRTEM) is an imaging mode of the transmission electron microscope (TEM) that allows the imaging of the crystallographic structure of a sample at an atomic scale. Because of its high resolution, it is an invaluable tool to study nano-scale properties of crystalline material such as semiconductors and metals. At present, the highest resolution realized is 0.8 angstroms (0.08 nm) with microscopes. Ongoing research and development such as efforts in the framework of TEAM will soon push the resolution of HRTEM to 0.5 Å. At these small scales, individual atoms and crystalline defects can be imaged. Since all crystal structures are 3-dimensional, it may be necessary to combine several views of the crystal, taken from different angles, into a 3D map. This technique is called electron crystallography. One of the difficulties with HRTEM is that image formation relies on phase-contrast. In phase-contrast imaging, contrast is not necessarily intuitively interpretable as the image is influenced by strong aberrations of the imaging lenses in the microscope. One major aberration is caused by focus and astigmatism, which often can be estimated from the Fourier transform of the HRTEM image.

Chapter 3

Results and Discussion

3.1 Effect of Supercritical Fluid and Post-Deposition Annealing on the ZrO₂/Ge MOS-Capacitor

This section we investigate the effect of Supercritical Fluid treatment (high-pressure H₂O treatment) on the sputter-deposition of ZrO₂/Ge stack. Then analysis of electrical characteristics can examine the quality of the treated device, and the material analysis of X-ray photoelectron spectroscopy (XPS) and high-resolution transmission electron microscopy (HRTEM) reveal the situation of interfacial GeO_x between ZrO₂ and Ge which is a redox of ZrO₂ with H₂O and GeO_x with H₂, including the bonding of Zr and Ge with O, and real thickness of GeO_x. The suppression of GeO_x interlayer between ZrO₂ and Ge substrate can decrease the gate leakage current effectively.

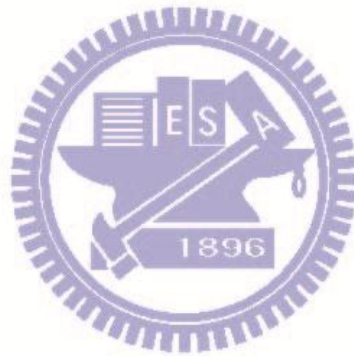
3.1.1 Thermal Stability of ZrO₂/Ge MOS-Capacitor

The thermal stability of MOS-C is the most important norm to referee quality of MOS-C. In the Fig. 3-1, it represents the variation of gate leakage current density (J_G) for ZrO₂ on Ge substrate after different thermal treatments. The symmetrical J_G of

ZrO₂ on p-type Ge substrate at negative and positive electrical field is due to fast generation rate of minority carrier. Furthermore, the J_G of ZrO₂/Ge capacitor decreases with increasing annealing temperature until 400 °C and then increases at 500 °C, as shown in Fig. 3-2. The high and unstable J_G of ZrO₂/Ge capacitor may be related to formation, decomposition and amalgamation of the Ge oxide during thermal process. The J_G comparison of depositing ZrO₂ on Ge has the same trend which the J_G increases after 500 °C thermal process due to the thermal decomposition GeO_x into dielectric.

The C-V characteristics of ZrO₂/Ge capacitor which treated by various thermal treatments are shown in Fig. 3-3 and the parameters are extracted in Table 3-1. The V_{fb}, Hysteresis, Thickness, CET and ε_{eff} present flat-band voltage, shift of flat-band voltage, thickness of ZrO₂ measured by n-k instrument, capacitance effective thickness and effective dielectric permittivity, respectively. We can know the lower accumulation capacitance in standard condition and 500 °C RTA-treated condition are attributed to the bad quality of ZrO₂ layer, because of its poor charge holding ability and cause high gate leakage, as shown in Fig. 3-3. Besides, the response of inversion capacitance at positive bias in 500 °C RTA-treated condition is expressed poor interface quality between ZrO₂ and Ge substrate. On the other hand, when temperature of thermal annealing is below 400 °C, the electrical performance of

ZrO₂/Ge capacitor is improved. But we know the activation temperature of source/drain annealing in the MOS process always be above 500 °C. Therefore, how to repair the thermal damage in gate dielectric and interface for Ge-based MOS device is necessary. So we bring up an idea about Supercritical Fluid treatment (high-pressure H₂O treatment) to repair the thermal damage of gate dielectric and interface.



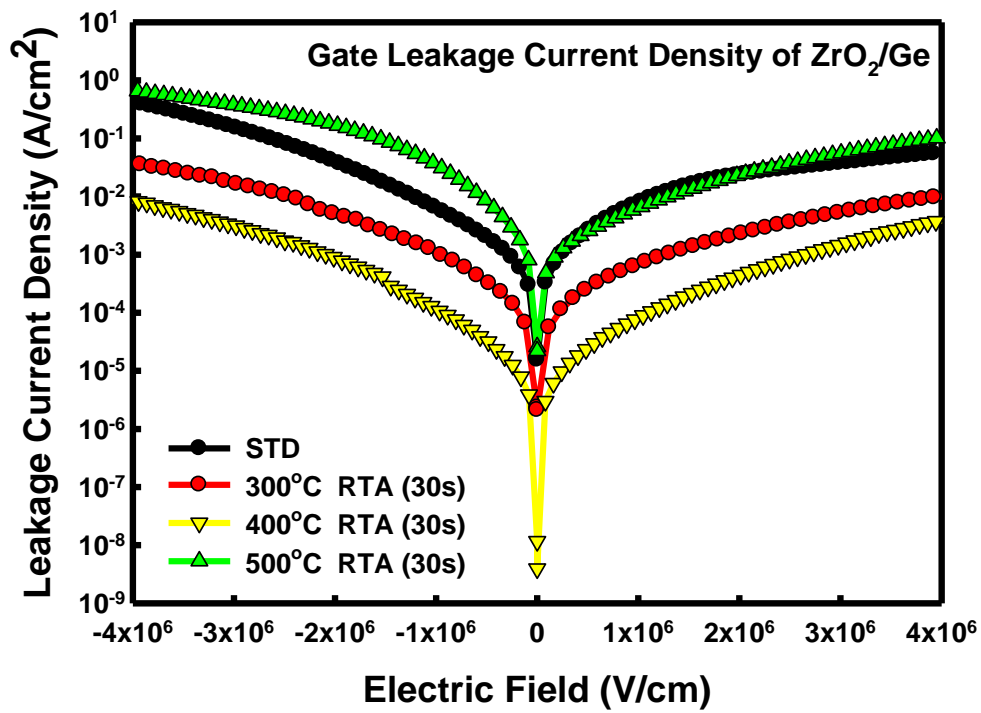


Fig. 3-1 The gate leakage current density of sputtered-ZrO₂ on Ge with various thermal treatments.

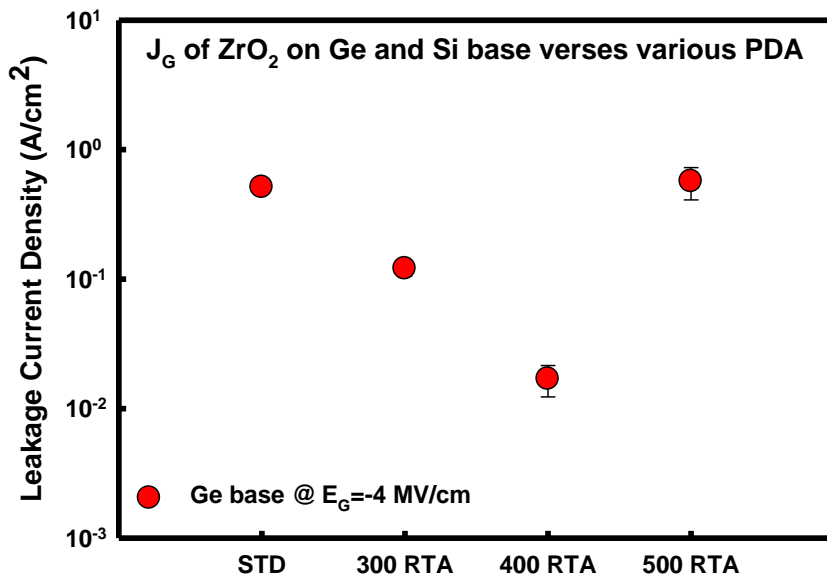


Fig. 3-2 The gate leakage current density of sputtered-ZrO₂ on Si with various thermal treatments.

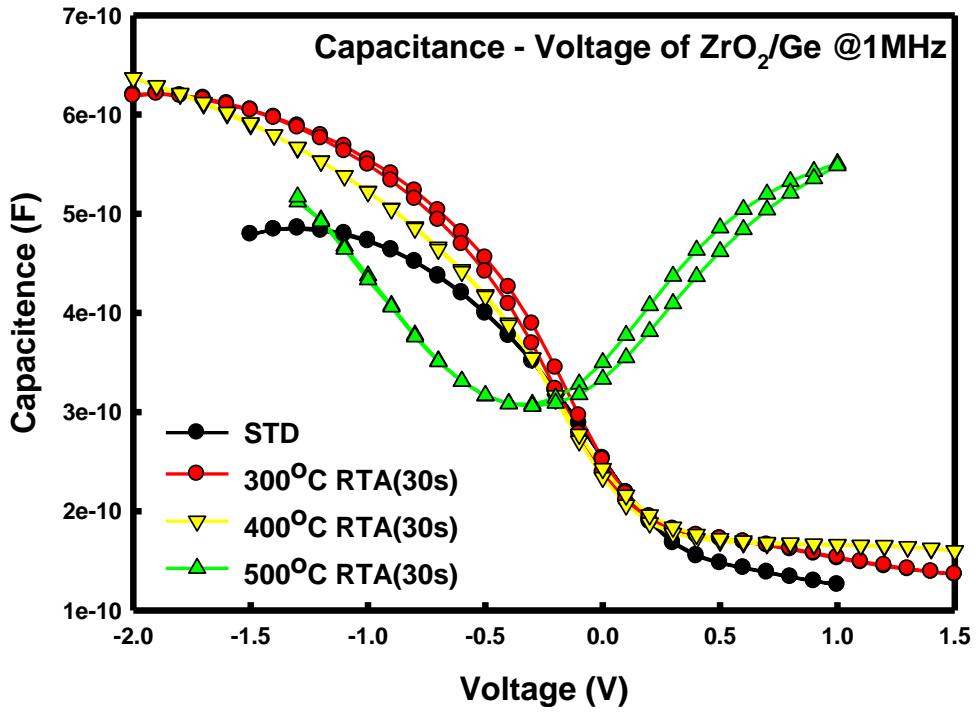


Fig. 3-3 The C-V characteristics of ZrO₂/Ge with various thermal treatments.

	STD	300°C RTA	400°C RTA	500°C RTA
V _{fb} (V)	-0.13	-0.09	-0.26	N/A
Hysteresis (V)	0.01	0.02	0.02	N/A
CET (nm)	2.04	1.40	2.17	1.97
Thickness (nm)	9	N/A	N/A	7.5
ε _{eff}	17.23	N/A	N/A	14.85

Table 3-1 The parameter of C-V characteristics for ZrO₂/Ge with various thermal treatments.

3.1.2 Effect of Supercritical Fluid Treatment on ZrO₂/Ge MOS-C

To repair the thermal damage in gate dielectric and interface for Ge-based MOS device, we propose an idea about Supercritical Fluid Treatment (SCF) as high pressure water treatment. The purpose of our treatment will focus on the interface of ZrO₂/Ge device.

First, the electrical characteristics are shown in Fig. 3-4, presenting the J_G with and w/o SCF treatment after 500 °C RTA treatment (serious thermal damage). It surely works to decrease the gate leakage about 3 orders after 500 °C RTA thermal damage. The cross-sectional HRTEM images in Fig. 3-5 show the sputtered ZrO₂ on Ge substrate after high vacuum annealing treat at 250 °C w/o and with N₂ RTA at 500 °C for 30s, then in Fig. 3-6 show the sputtered ZrO₂ on Ge substrate after N₂ RTA treat at 500 °C for 30s w/o and with SCF treatment. After thermal process, the ZrO₂ film crystallizes clearly, and the thickness of GeO_x layer decrease with high temperature RTA. The 4 and 2.5 nm-thickness GeO_x layers are observed w/o and with RTA, respectively, and effect of the SCF treatment on GeO_x was discovered by HRTEM images in Fig. 3-6 (b) without GeO_x interfacial layer amazingly.

Second, from the Fig. 3-7 and Fig. 3-8, the XPS spectra of Ge 2p_{3/2} and Zr 3p_{3/2} shows the bonding situations and composition respectively. We detect that the

reaction between ZrO_2 and GeO_x is existent during RTA and SCF treatment. The Ge $2p_{3/2}$ peak at binding energies about 1217 eV and 1219.4 eV are associated with pure Ge and GeO_x , respectively, shown in Fig. 3-7.^[30] And the interfacial layer of STD and 500 °C RTA treated is almost GeO_x , but it will be removed after SCF treatment. Then, the Zr $3p_{3/2}$ peak at a binding energy about 332.5 eV is associated with ZrO_2 , and shown in Fig. 3-8. The peak of Zr $3p_{3/2}$ signal which is treated by SCF treatment shift to higher binding energy as the Ar^+ sputtering time increases, but not obvious in the STD and RTA-treated condition.

Base on the previous evidences, we can know that the zirconia will be oxidized more when the GeO_x eliminated by SCF treatment, and cause J_G decrease. For the elimination of GeO_x layer, it called reduction of GeO_x . The redox may occur at the interface between ZrO_2 and GeO_x during SCF treatment, as follows:



The reactions imply the H_2O is taken as oxidant and reacts with the non-oxidized Zr in the interlayer and the GeO_x dissolved after SCF treatment. The amounts of ionic products which are like H_3O^+ and OH^- radicals in H_2O at high pressure may higher than those obtained in atmospheric pressure. The higher amounts of free radicals are associated with a strengthened oxidation reaction between H_2O and non-oxidized Zr

owing to the higher collision frequency, as Eq. (3-1).^[31] Besides, the generation of hydrogen using Zr and H₂O has also been reported.^[32] The existence of H₂, the reaction of Eq. (3-2) proceeds spontaneously ($\Delta G=-42.69$ kJ/mol at 100°C) and reduces the GeO_x to Ge.^[33] In addition, Zr oxidation reacts easily at the interface of ZrO₂/Ge due to the H₂ is effectively removed by GeO_x. Therefore, SCF treatment can eliminate the interfacial GeO_x layer in the ZrO₂/Ge effectively. The transporting mechanism of SCF elements may diffuse through the grain boundary of poly-type ZrO₂ film, as the Fig. 3-9, and the schematic diagram of GeO_x reduction reactions is in the Fig. 3-10.

In the end, it's clearly to know the reduction of GeO_x by depth profiles of Zr, O and Ge atoms in Fig. 3-11 to Fig. 3-13. The depth profiles are analyzed by collecting XPS signals with various Ar⁺ sputtering time. Signals of O 1s, Zr 3p_{3/2} and Ge 2p_{3/2} were collected to calculate the atom %. From the Fig. 3-11 to Fig. 3-13, the amount of GeO_x decrease by thermal process which the following RTA in N₂ ambient at 500 °C for 30s. This is the thermal decomposition of GeO_x when the temperature of annealing is higher than 420 °C.^[34] In the Fig. 3-13, we know SCF treatment can cause the interfacial GeO_x signal to vanish and reduced the amount of GeO_x that was incorporated into the ZrO₂ thin film. So, the SCF treatment can eliminate the amount of GeO_x and help to reduce the gate leakage current, as shown in the Fig. 3-4.

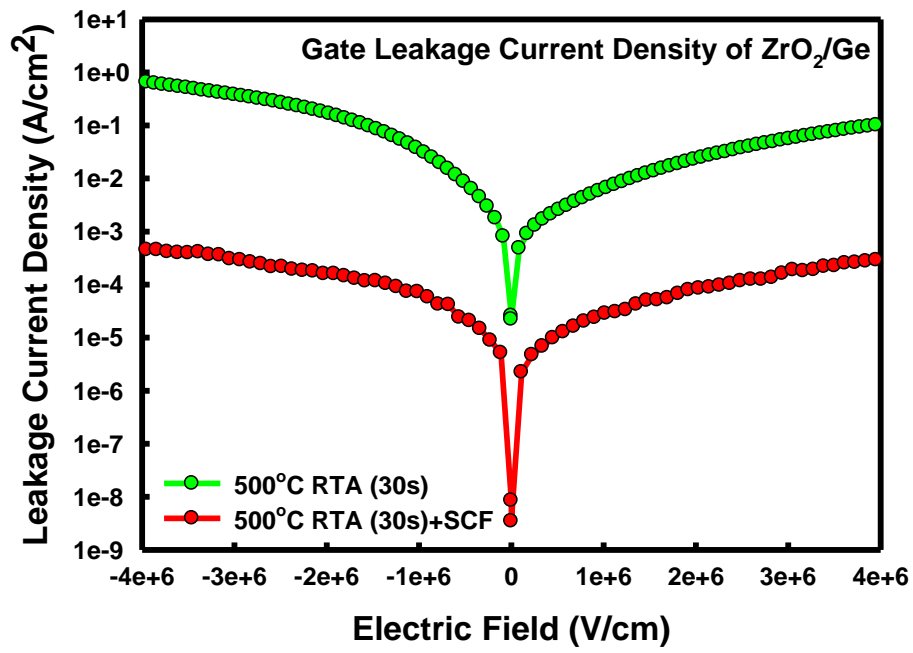
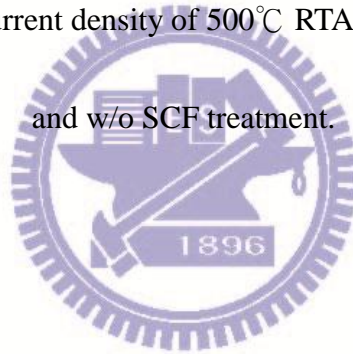


Fig. 3-4 The gate leakage current density of 500°C RTA-treated condition on Ge with and w/o SCF treatment.



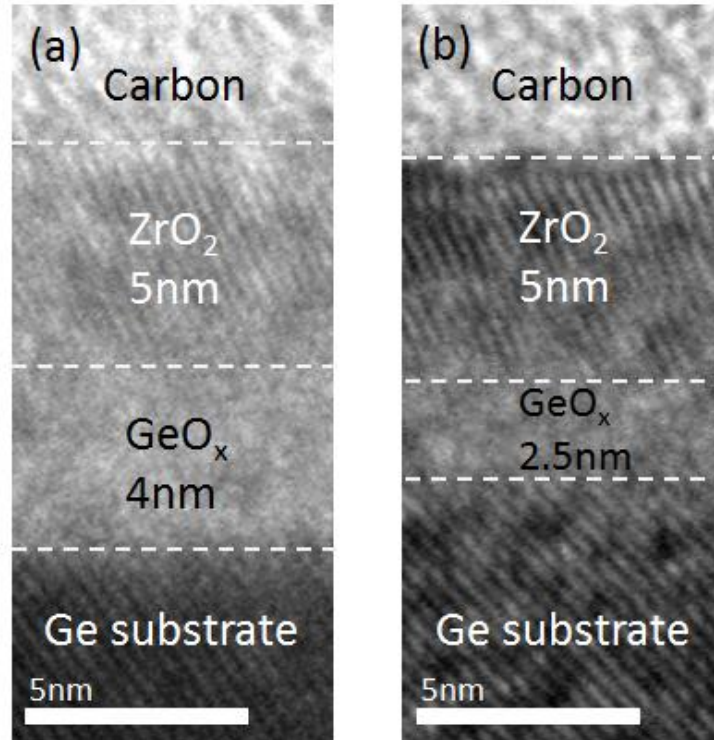


Fig. 3-5 The cross-sectional HRTEM images of sputtered-ZrO₂ on Ge with high vacuum annealing at 250 °C (a) w/o and (b) with RTA treatment at 500 °C.

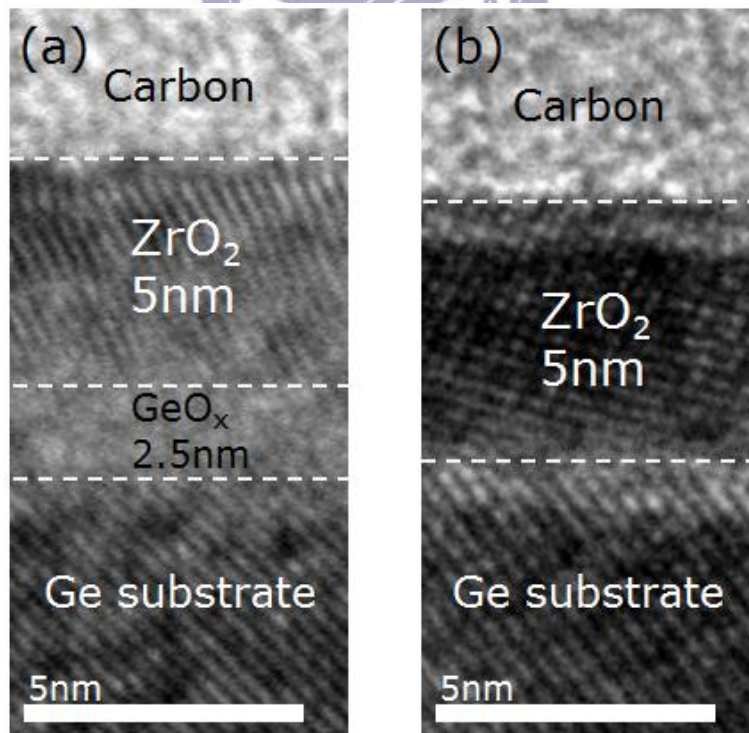


Fig. 3-6 The cross-sectional HRTEM images of sputtered-ZrO₂ on Ge with high vacuum annealing at 250 °C and 500 °C RTA (a) w/o and (b) with SCF treatment.

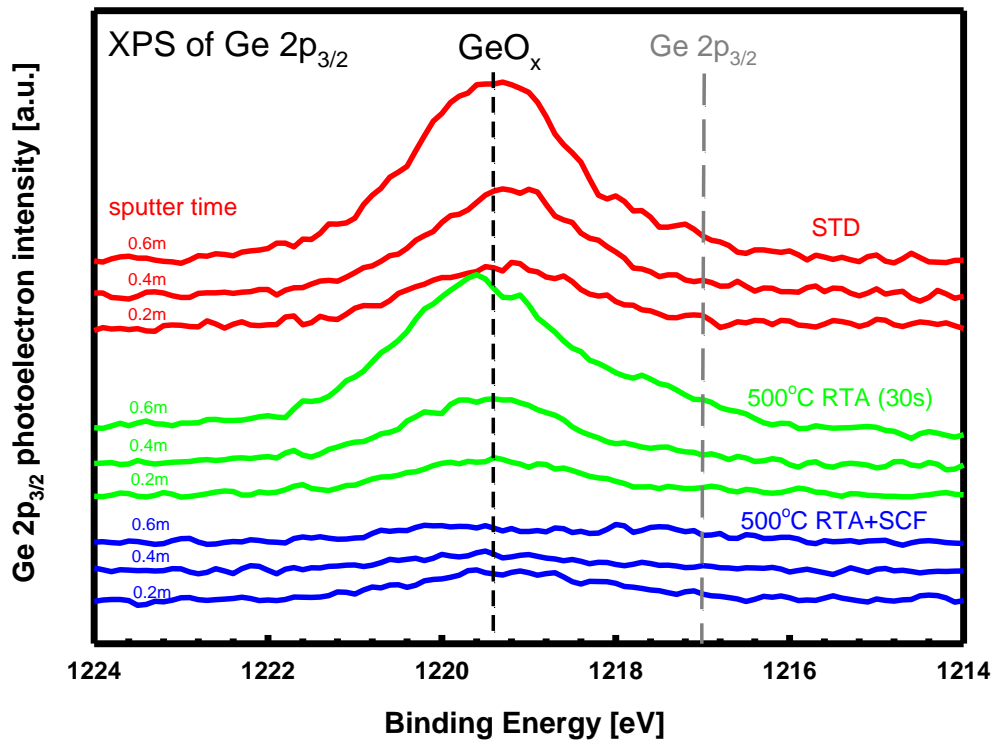


Fig. 3-7 The XPS spectra of Ge $2p_{3/2}$ with various treatments.

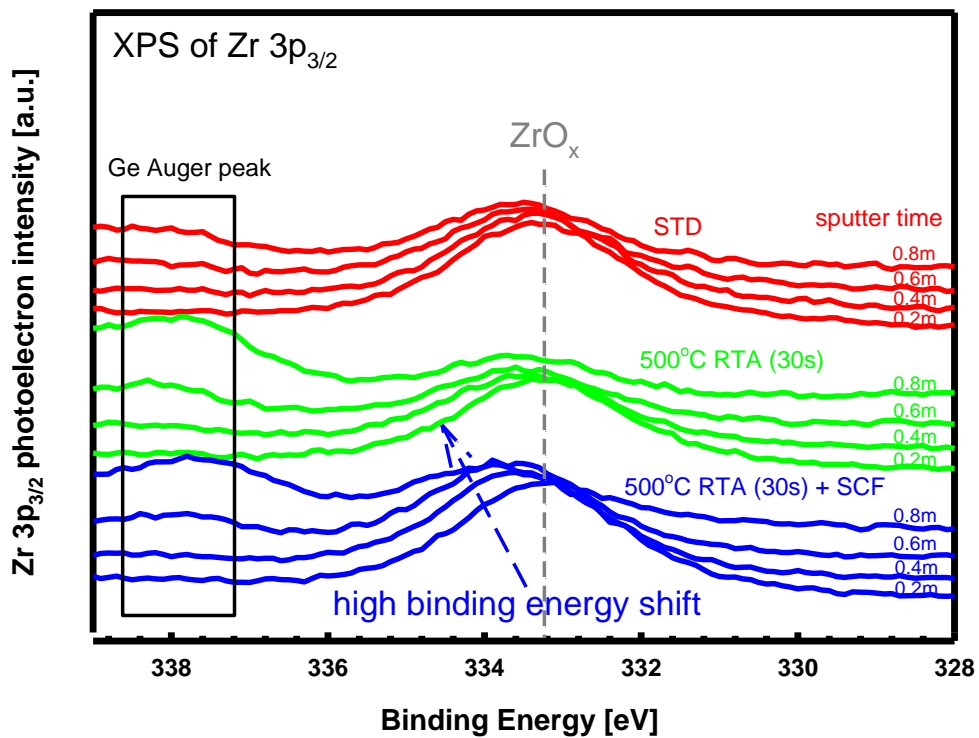


Fig. 3-8 The XPS spectra of Zr $3p_{3/2}$ with various treatments.

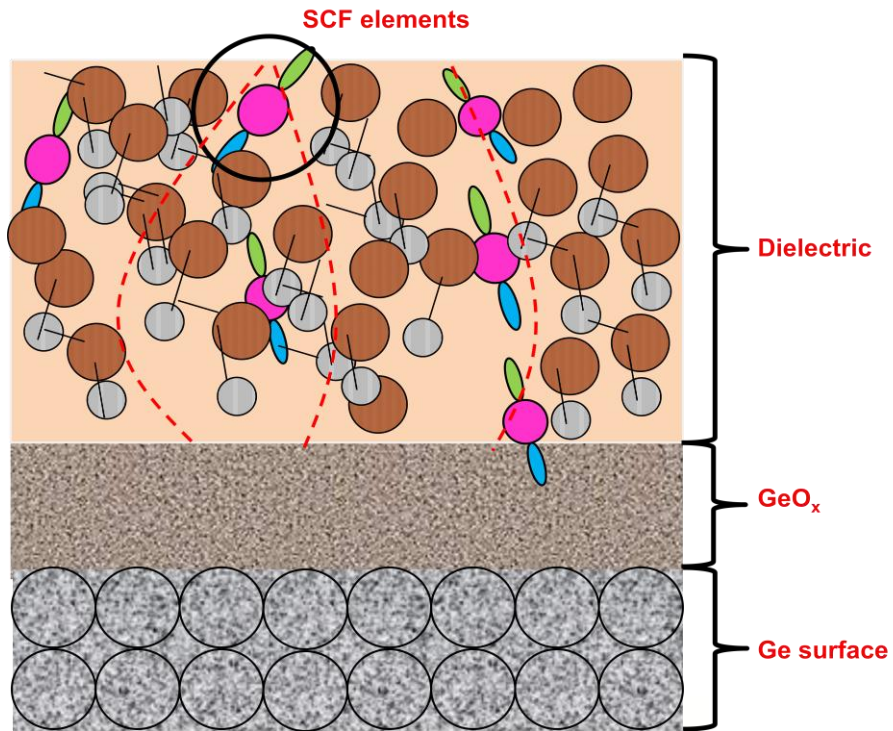


Fig. 3-9 The transporting mechanism for SCCO₂ fluids taking H₂O molecule into dielectric film.

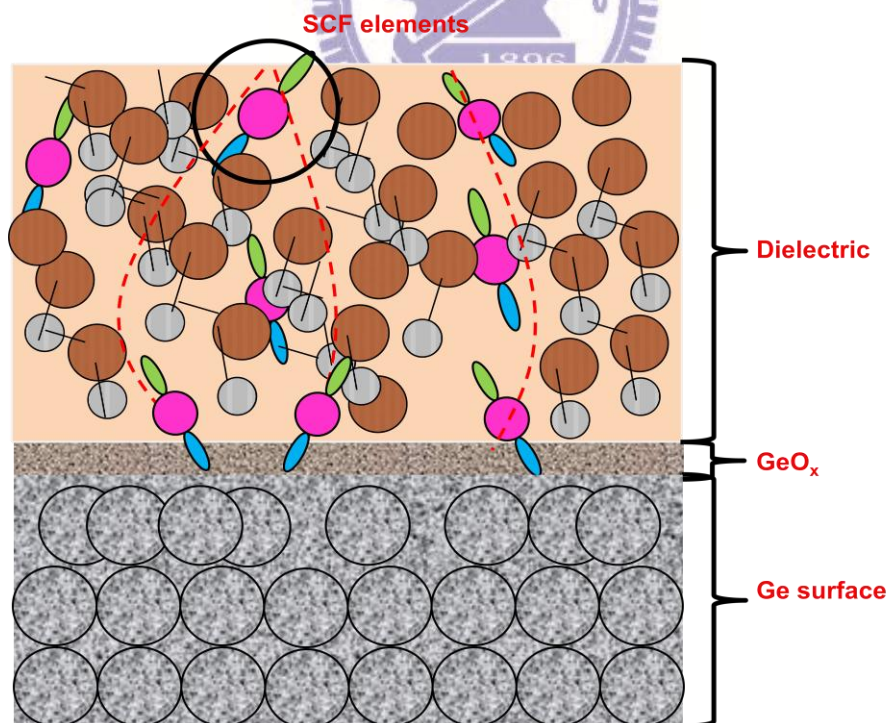


Fig. 3-10 The schematic diagram of GeO_x reduction reactions on the interfacial layer.

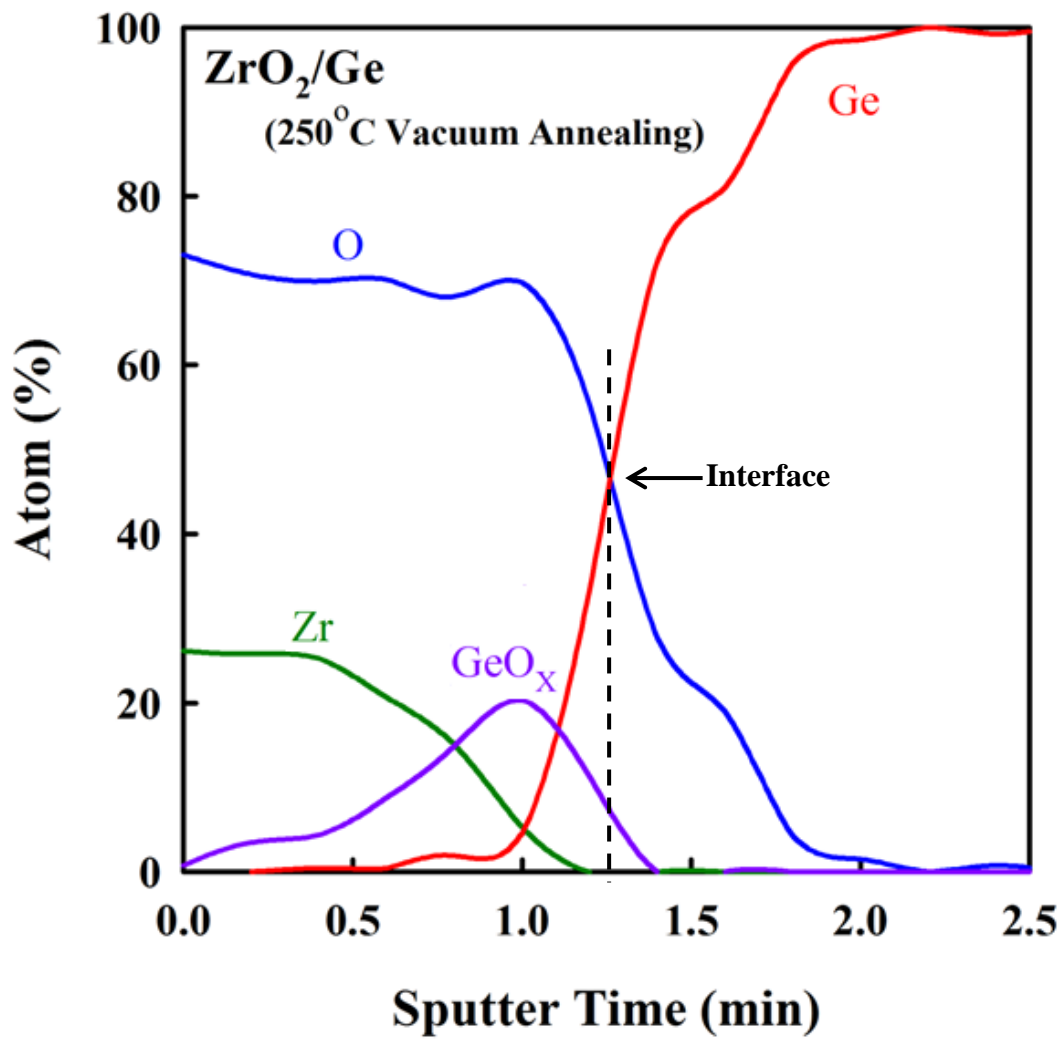


Fig. 3-11 Depth profiles of Zr, O and Ge atoms in ZrO₂/Ge after high vacuum annealing at 250 °C for 30 min by XPS.

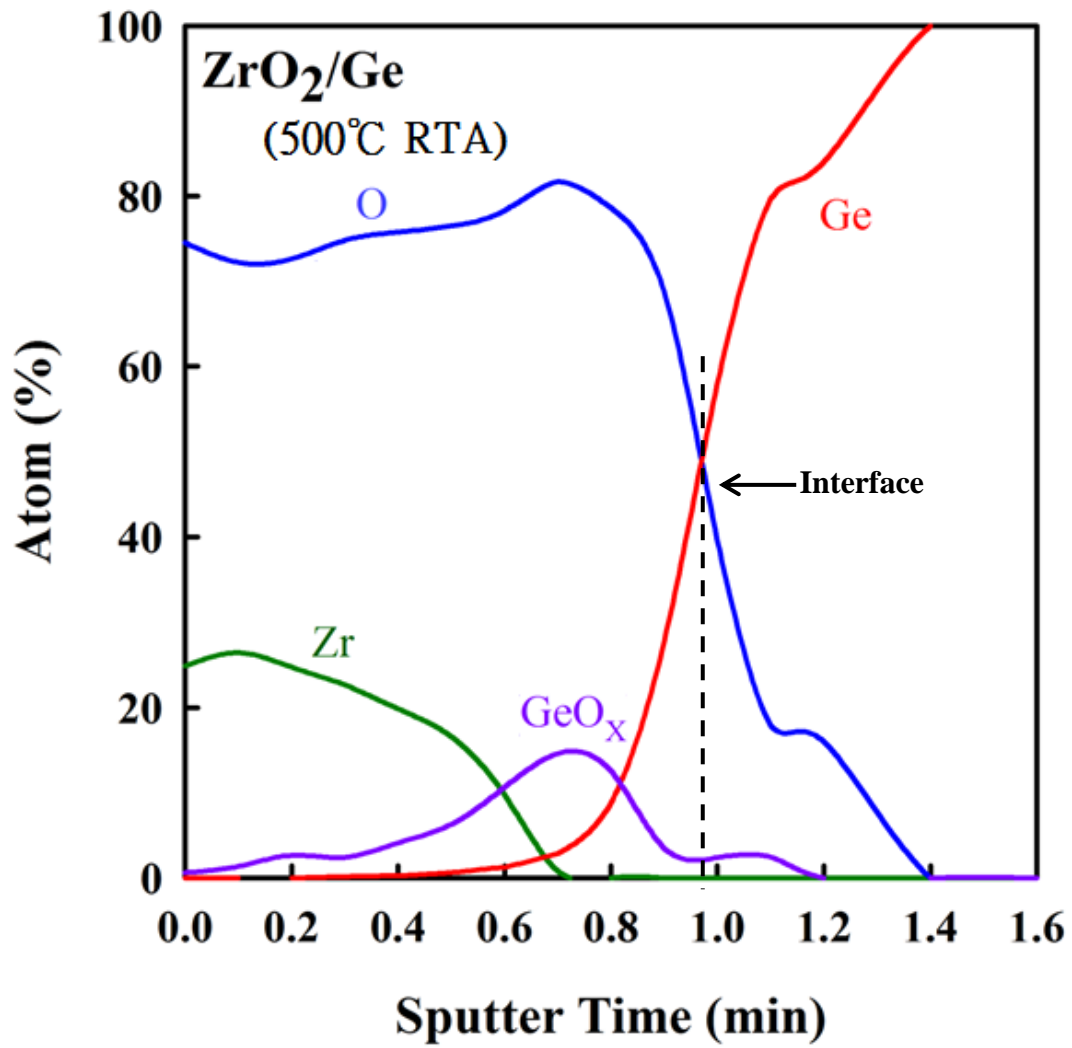


Fig. 3-12 Depth profiles of Zr, O and Ge atoms in ZrO₂/Ge after high vacuum annealing at 250 °C for 30min and 250 °C RTA for 30sec by XPS.

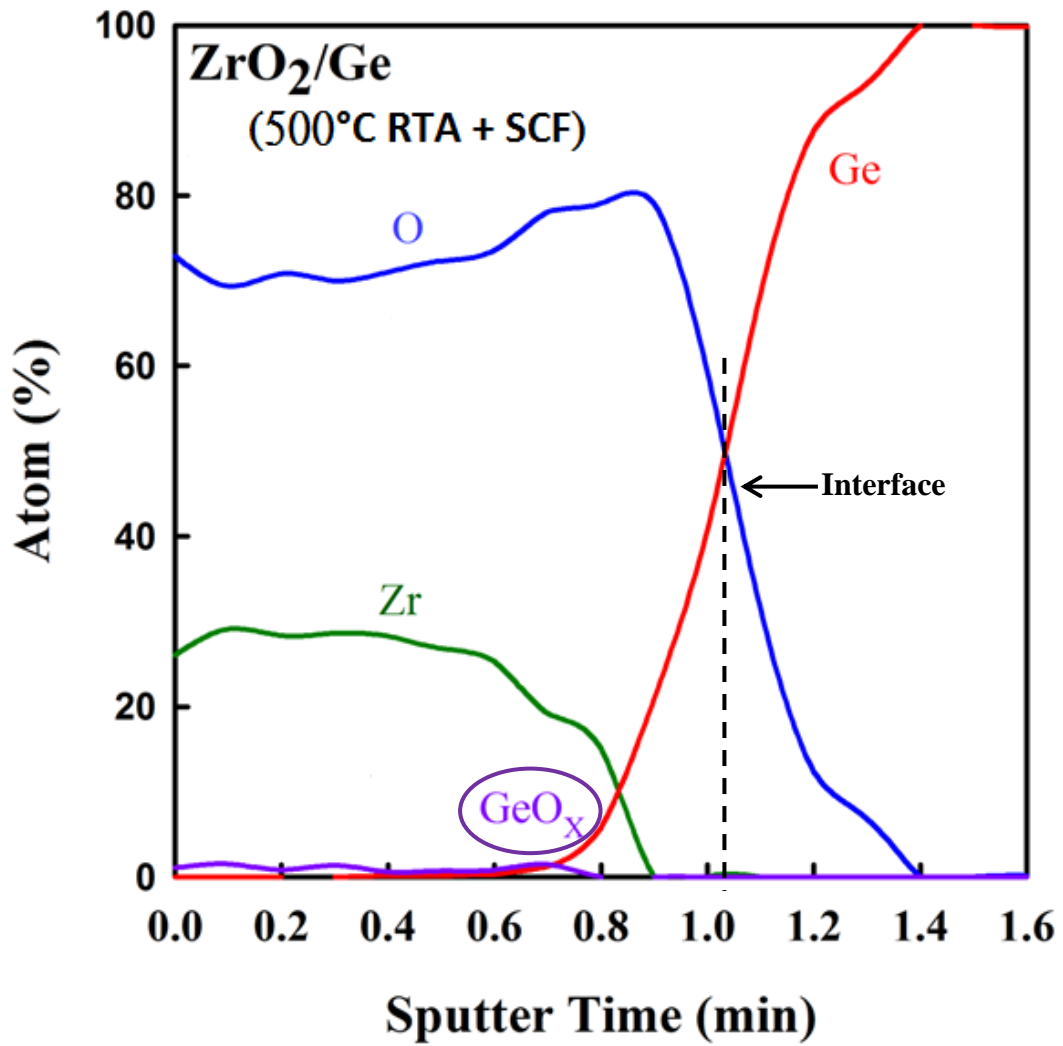


Fig. 3-13 Depth profiles of Zr, O and Ge atoms in ZrO₂/Ge after high vacuum annealing at 250 °C for 30 min, 250 °C RTA for 30sec and SCF for 60min by XPS.

3.2 Effect of Water Vapor Annealing on the ZrO₂/Ge MOS-Capacitor

Continued from the preceding section, this section we investigate the effect of Water Vapor Annealing (atmospheric pressure H₂O treatment) on the sputter-deposition of ZrO₂/Ge stack. The differences between Water Vapor Annealing and Supercritical Fluid Treatment are different treated pressure and temperature. After suitable annealing temperature with water vapor, it can also reduce GeO_x layer and repair the defect which formed by reduction of GeO_x effectively. And then analysis of electrical characteristics can examine the quality of the treated device, and the material analysis of X-ray photoelectron spectroscopy (XPS) reveal the situation of interfacial GeO_x between ZrO₂ and Ge which is a redox of ZrO₂ with H₂O and GeO_x with H₂, including the bonding of Zr and Ge with O, and real thickness of GeO_x.

3.2.1 Compare with Water Vapor Annealing and Nitrogen Annealing

After Supercritical Fluid Treatment (SCF), it may leave many defects on the interface of ZrO₂/Ge and cause poor C-V characteristics. To solve this problem, we propose an idea about water treatment with suitable temperature (below 420°C), called Water Vapor Annealing. The purpose of our treatment will focus on the repair

of ZrO₂/Ge interface.

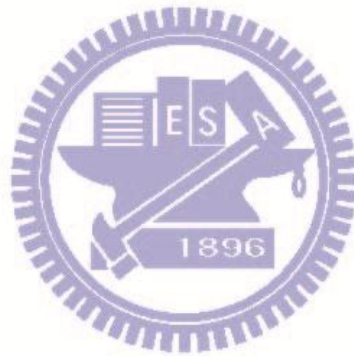
First, the electrical characteristics are shown in Fig. 3-14, presenting the J_G with Water Vapor Annealing and Dry Nitrogen Annealing at 300 °C for 3min. The J_G of H₂O+N₂ 300 °C RTA is lower than dry N₂ 300 °C RTA, because the suppression of the GeO_x causes fewer interface traps.^[23] In the C-V characteristics, they are shown in Fig. 3-17. The accumulation capacitance of H₂O+N₂ RTA is higher than dry N₂ RTA at 300°C, because of the H₂O+N₂ 300 °C RTA can reduce the GeO_x layer and the total thickness is thinner than dry N₂ 300 °C RTA. Besides, from slope of the depletion capacitance, the slope of H₂O+N₂ 300 °C RTA is sharper than dry N₂ 300 °C RTA, it indicates the interface quality of H₂O+N₂ 300 °C RTA is better than dry N₂ 300 °C RTA, and this should be attributed to the suppressed growth of the unstable GeO_x interlayer by water treatment. As the following material analysis, there is more evidence to prove the water treatment can suppress the growth of the unstable GeO_x interlayer and form superior bulk and interface properties.

Second, from the Fig. 3-16 and Fig. 3-17, the XPS spectra of Ge 2p_{3/2} and Zr 3p_{3/2} shows the bonding situations and composition respectively. We detect that the reaction between ZrO₂ and GeO_x is existent during 300°C H₂O+N₂ and dry N₂ RTA. The Ge 2p_{3/2} peaks of 300°C H₂O+N₂ RTA and dry N₂ RTA at binding energies about 1217 eV and 1219.4 eV are associated with pure Ge and GeO_x, respectively, shown in

Fig. 3-16. The ratio of GeO_x treated by dry N_2 RTA is higher than $\text{H}_2\text{O}+\text{N}_2$ RTA, and it means H_2O treatment can eliminate GeO_x layer. Comparing with SCF and $\text{H}_2\text{O}+\text{N}_2$ RTA, it's clear to know high pressure water treatment can eliminate GeO_x layer effectively than atmospheric pressure water treatment, so the redox of water in high pressure is more efficacious than in atmospheric pressure. And a lot of defects in the GeO_x layer will cause the high gate leakage, showed as the J_G of $\text{H}_2\text{O}+\text{N}_2$ 300 °C RTA is lower than dry N_2 300 °C RTA. ^[23] Then, the Zr $3p_{3/2}$ peak at a binding energy about 332.5 eV is associated with ZrO_2 , and shown in Fig. 3-17. The peak of Zr $3p_{3/2}$ signals which is sample treated by $\text{H}_2\text{O}+\text{N}_2$ 300 °C RTA shift to higher binding energy as the Ar^+ sputtering time increases, but not obvious in the STD and dry N_2 300 °C RTA condition. It means that un-bonding Zr will oxidize by with the water treatment, so water treatment will cause redox surely.

In the end, it's clearly to know the reduction of GeO_x by depth profiles of Zr, O and Ge atoms in Fig. 3-18, Fig. 3-19 and Fig. 3-20. The depth profiles are analyzed by collecting XPS signals with various Ar^+ sputtering time. Signals of O 1s, Zr $3p_{3/2}$ and Ge $2p_{3/2}$ were collected to calculate the atom %. From the Fig. 3-18 to Fig. 3-20, the amount of GeO_x decrease by $\text{H}_2\text{O}+\text{N}_2$ 300 °C RTA for 3min, but not dry N_2 300 °C RTA. In the Fig. 3-19, we know water treatment can reduce the amount of GeO_x interfacial layer, and it can help to repair the interface after annealed by suitable

temperature, showed as C-V characteristics in Fig. 3-15. So, the SCF treatment can eliminate the amount of GeO_x more effectively and help to reduce the gate leakage current, and the Water Vapor Annealing can repair the interface of ZrO_2/Ge .



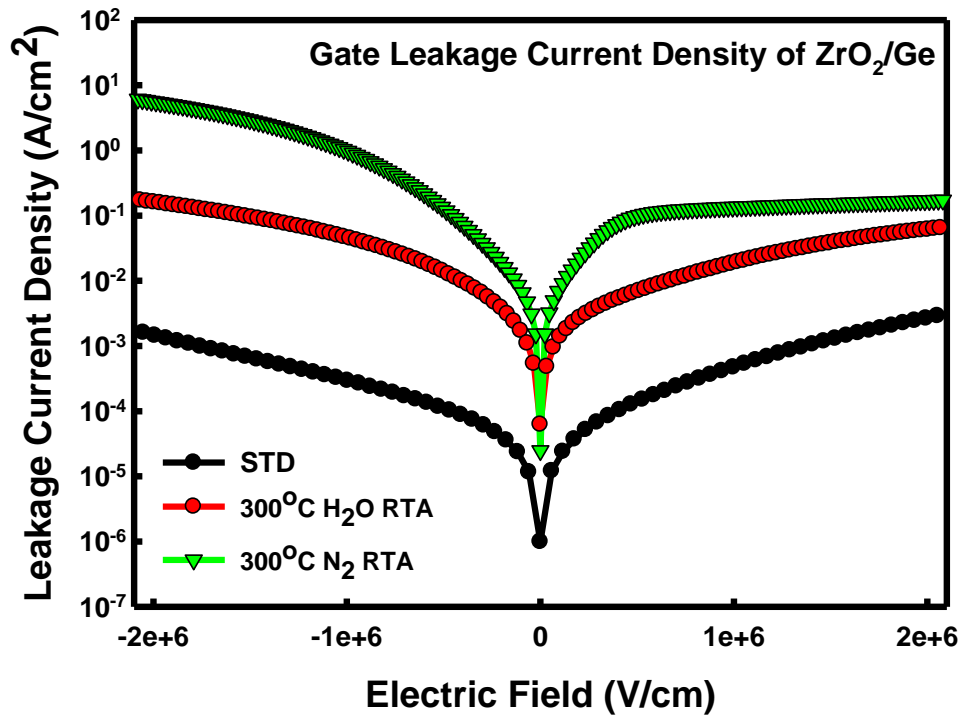


Fig. 3-14 The gate leakage current density of ZrO₂/Ge with 300°C H₂O and N₂ RTA.

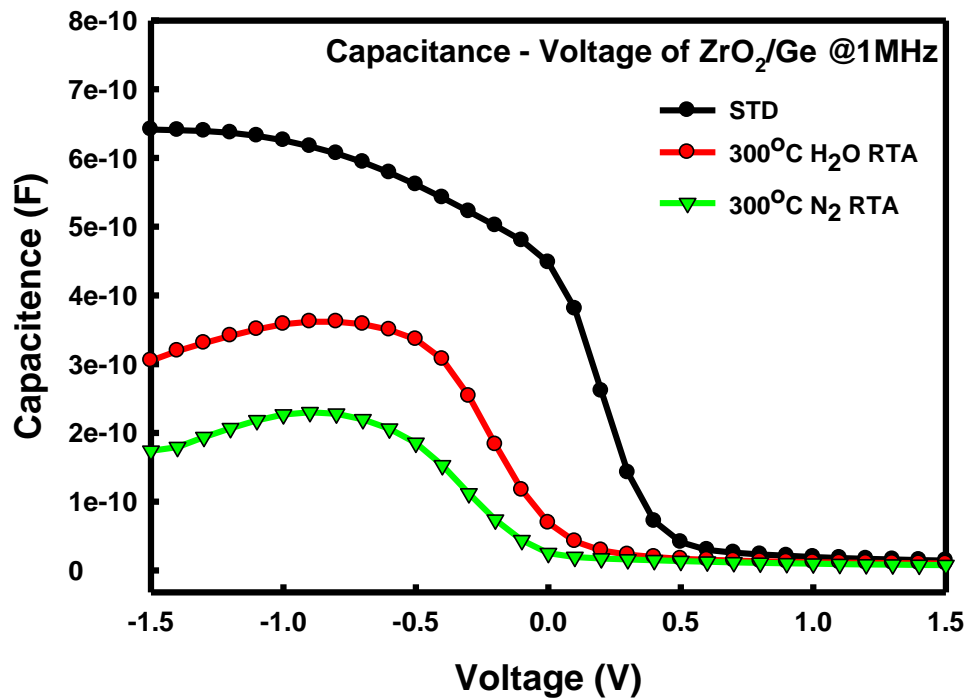


Fig. 3-15 The C-V characteristics of ZrO₂/Ge with 300°C H₂O and N₂ RTA.

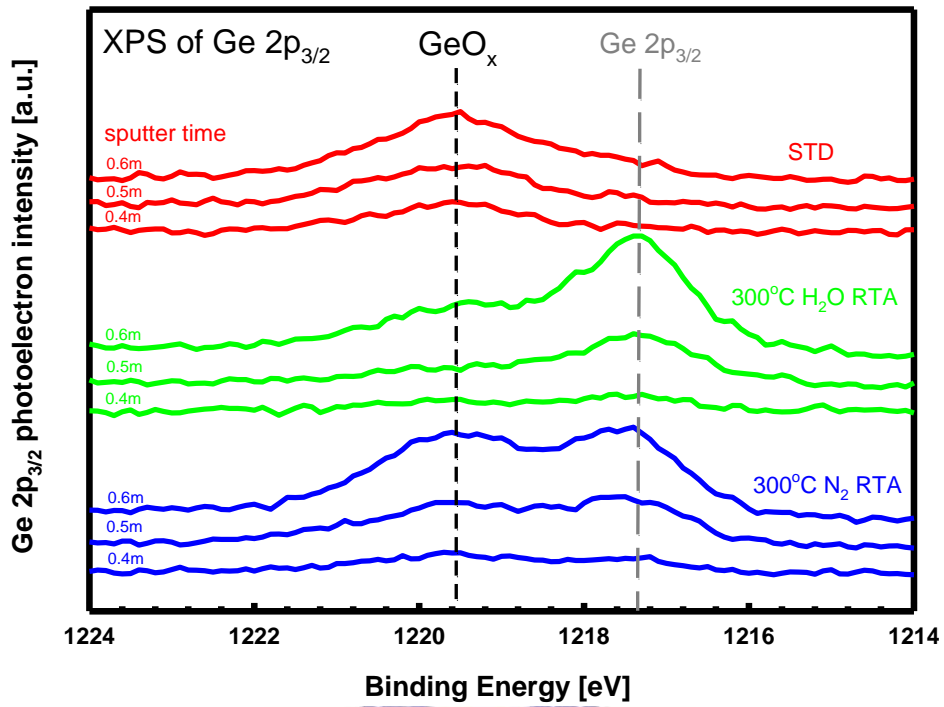


Fig. 3-16 The XPS spectra of Ge $2p_{3/2}$ with 300°C H₂O and N₂ RTA.

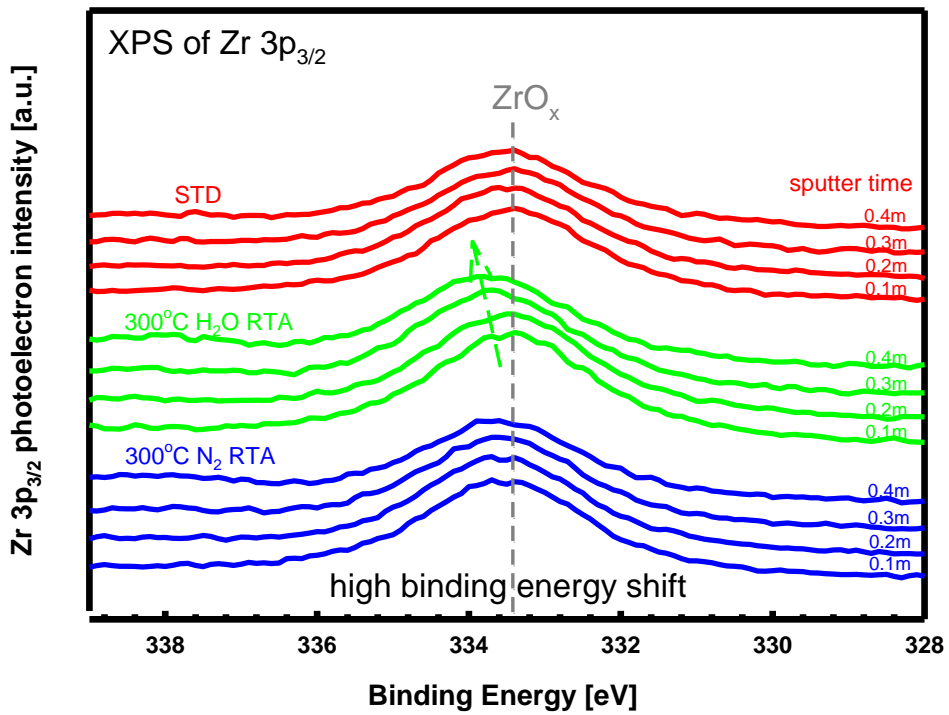


Fig. 3-17 The XPS spectra of Ze $3p_{3/2}$ with 300°C H₂O and N₂ RTA.

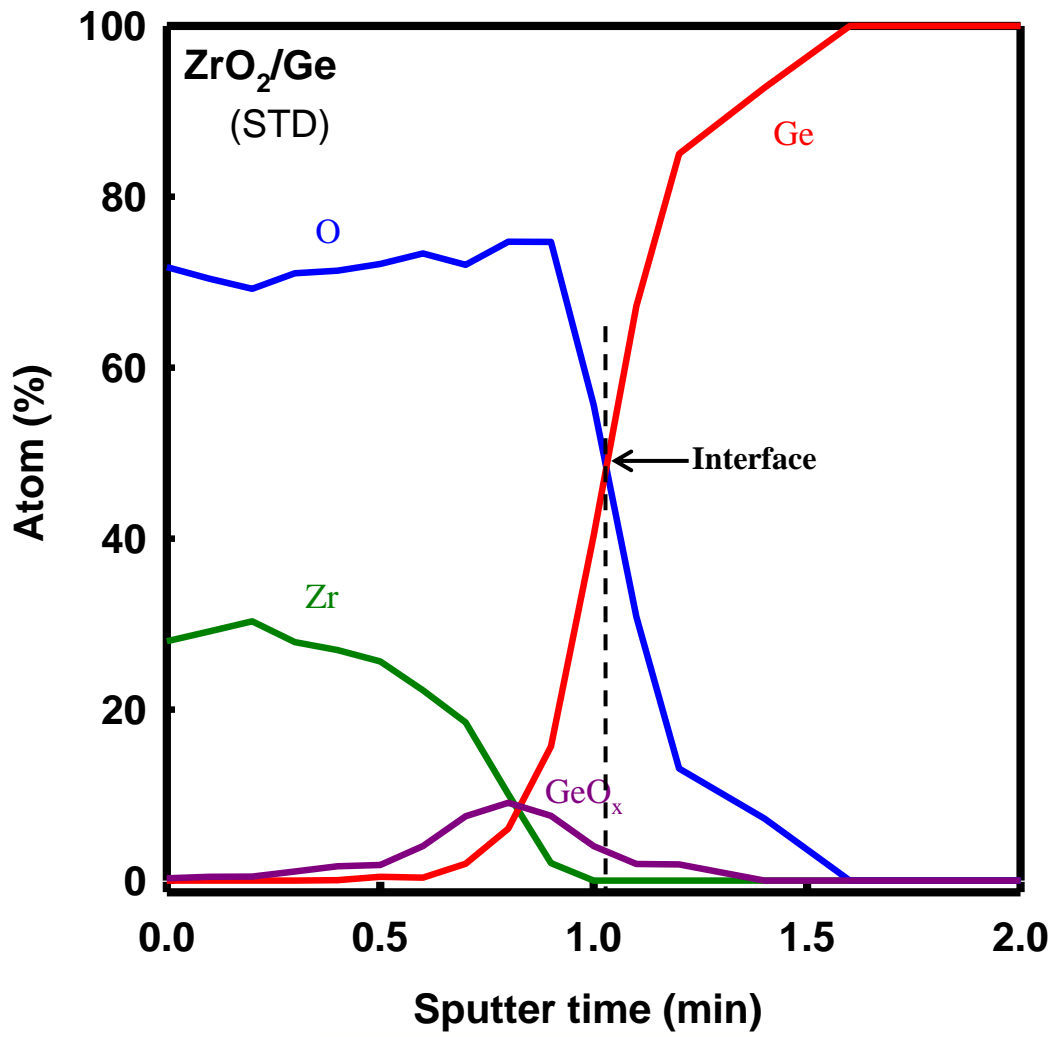


Fig. 3-18 Depth profiles of Zr, O and Ge atoms in ZrO_2/Ge with STD condition by XPS.

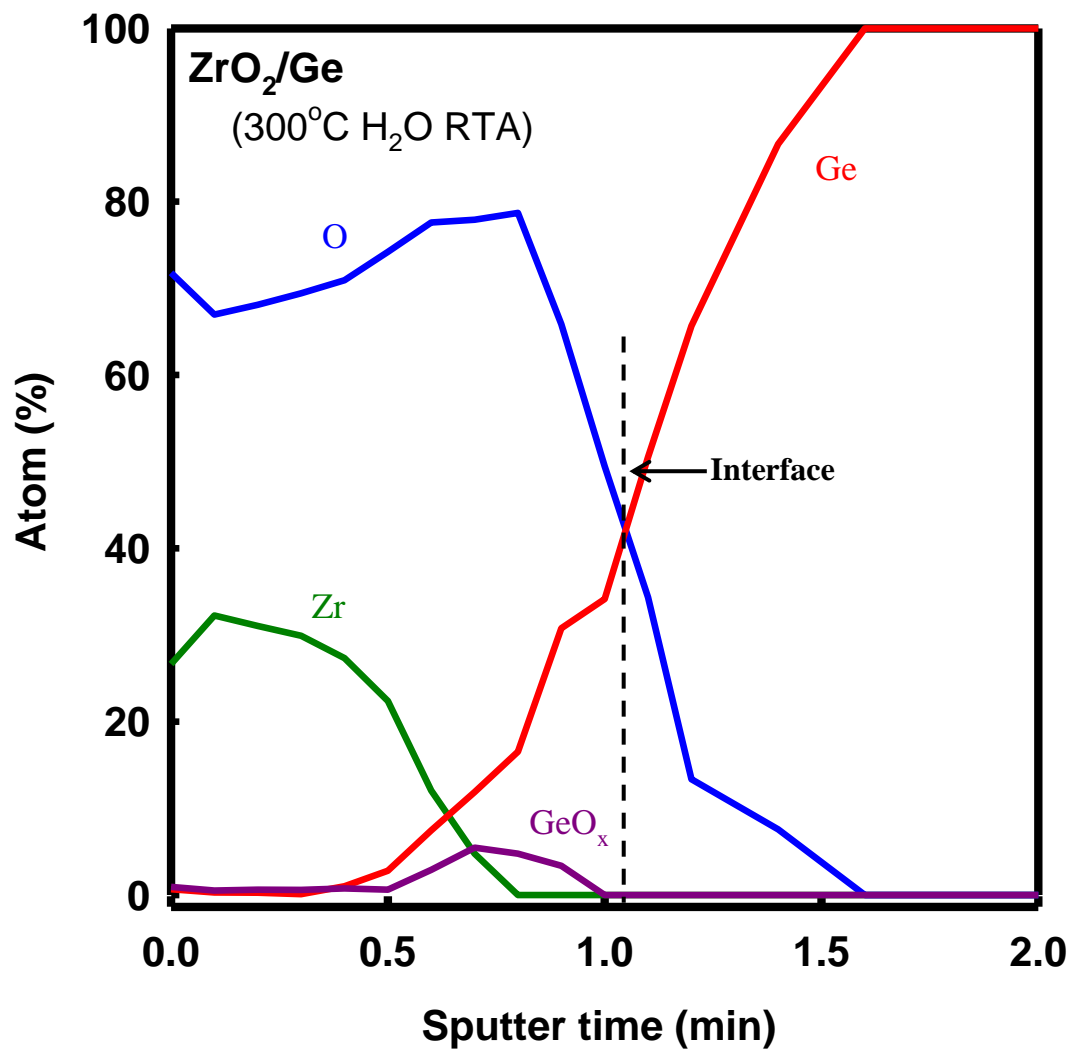


Fig. 3-19 Depth profiles of Zr, O and Ge atoms in ZrO₂/Ge with Water Vapor

Annealing at 300 °C for 3 mins by XPS.

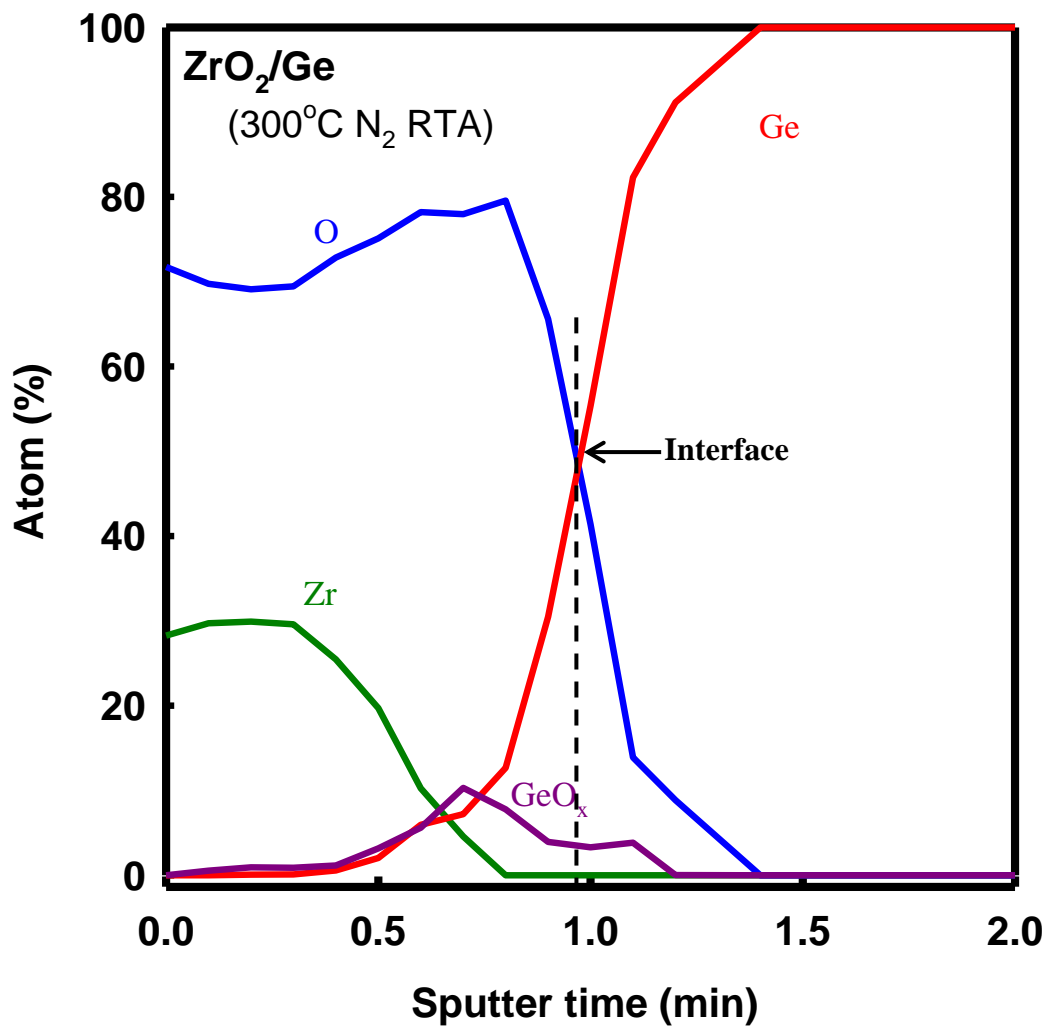


Fig. 3-20 Depth profiles of Zr, O and Ge atoms in ZrO₂/Ge with Dry Nitrogen
 Annealing at 300 °C for 3 mins by XPS.

3.2.2 Combination of Supercritical Fluid and Water Vapor Annealing

Continued from the preceding sections, the water treatment is effective in reduction of GeO_x , and through suitable annealing temperature can repair the defect of interface by reducing GeO_x . In the Fig. 3-21, it shows that the accumulation capacitance of sample treated by SCF and Water Vapor Annealing will return to STD, and more higher than treated by Water Vapor Annealing only. Therefore, the SCF can reduce the GeO_x effectively but it also leave defect on the interface, and cause the poor C-V characteristic. To solve this problem the Water Vapor Annealing is good for repair the interface by suitable temperature (below 420°C), and the water can also prevent the production of GeO_x , so the C-V characteristic can return to STD after thermal treatment. In addition, the SCF can enhance the electric characteristic obviously after the thermal process only, and it doesn't work without any thermal process first due to the degree of dielectric crystallization. The degree of dielectric crystallization may help the SCF element diffuse into dielectric more easily.

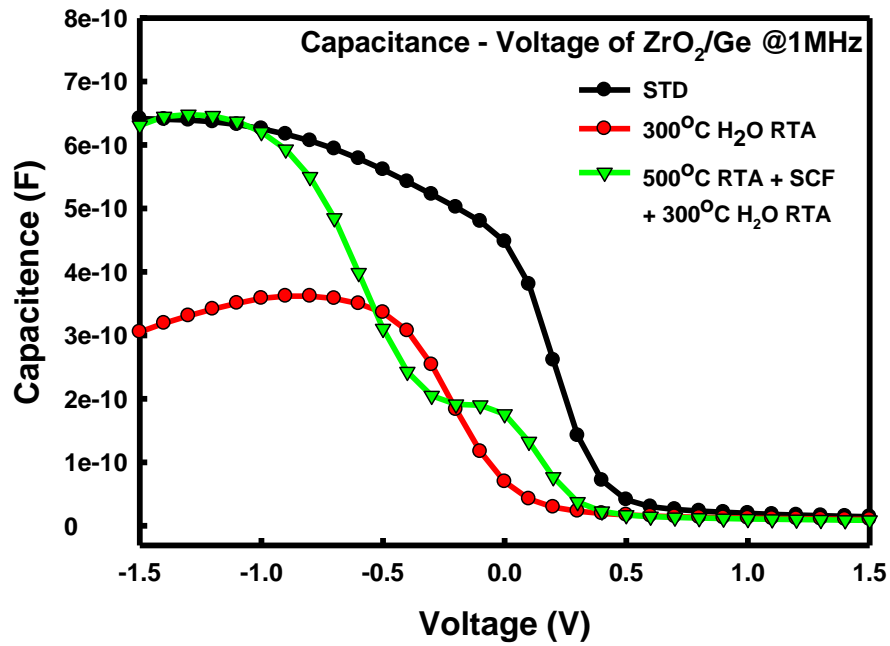
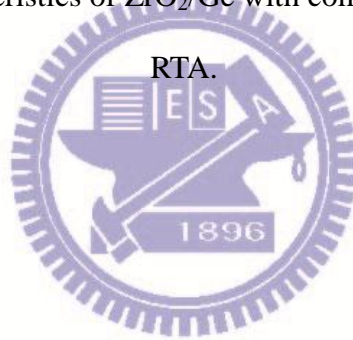


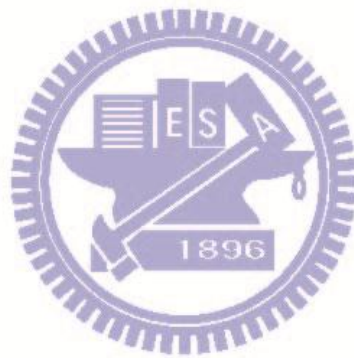
Fig. 3-21 The C-V characteristics of ZrO₂/Ge with combining SCF and 300°C H₂O



3.3 Summaries

In the summary, the growth of the unstable GeO_x interlayer by the thermal process can be suppressed by the water treatment. No matter the water at high pressure or atmospheric pressure, it all can eliminate the GeO_x interlayer and suppress the growth of GeO_x. But it's clear to know the pressure of the water treatment effect the capability of redox. In terms of the depth profiles analyzed by XPS and HRTEM images, the amount of GeO_x by treating with high pressure water treatment is less than treating with atmospheric pressure. Therefore, the high pressure water treatment

can reduce the gate leakage current effectively, and annealing with the suitable temperature can also repair the defect of interface.



Chapter 4

Conclusions and Future works

4.1 Conclusions

In this study, to solve the thermal decomposition of GeO_x the high pressure water treatment (supercritical fluids technology) is employed originally to eliminate the GeO_x interlayer and improve the properties of ZrO_2 high-k film. First, the thermal stability of ZrO_2/Ge stack is analyzed by the sample treated with 250°C high vacuum furnace annealing for 30min and then treated by 300°C , 400°C and 500°C N_2 RTA for 30s respectively. Second, the high pressure water treatment (SCF) at 100°C and 3000psi for 1hr used to the sample which is treated by 500°C N_2 RTA for 30s. By HR-TEM, XPS analyses, it can verify the elimination of GeO_x interlayer due to the SCF treatment surely, and explain the improvement of the gate leakage after SCF treatment. We also indicate the mechanism about the reduction of GeO_x interlayer in ZrO_2/Ge by SCF treatment, including the oxidation of un-bonding Zr and reduction of GeO_x . The reduction of GeO_x layer at the ZrO_2/Ge interface can reduce the interface defects and cause the gate leakage decrease. Besides, the Water Vapor Annealing is used to verify the water treatment has the ability of redox in the ZrO_2/Ge stack, and

though the annealing by suitable temperature can repair the interface to improve the electric characteristic of ZrO_2/Ge device.

The water treatment with suitable annealing temperature is the attractive technology to apply on Ge-typed MOS devices process. It's useful to resolve the GeO_x thermal decomposition issues to repair the interface of device which treated by thermal process and fabricate the high quality Ge-typed MOS devices.

4.2 Future works

To complete the high quality Ge-MOSFET, metal gate is another issue on the germanium devices. The work function tuning is a key to determined threshold voltage, however, for Ge-MOSFET, Fermi level pinning is the problem on metal gate/high-k/Ge MOS stack devices, which is waiting to be solved.

The feasibility of SCF can join the suitable temperature (below $400^\circ C$), and two step annealing to form the good interface, no GeO_x interlayer and good dielectric quality of high-k/Ge MOS stack. First, low temperature (below $300^\circ C$) annealing with high vacuum system. Second, after high temperature process, SCF treatment with suitable annealing temperature can eliminate the GeO_x interlayer which formed by thermal process and form a good interface.

Reference

- [1] S. M. Sze, and Kwok K. Ng, *Physics of Semiconductor Devices 3rd*.
- [2] E. J. Nowak, *IBM J. Res. & Dev. Vol. 46 No. 2/3*, 2002.
- [3] K. Rim, S. Koester, M. Hargrove, J. Chu, P. M. Mooney, J. Ott, T. Kanarsky, P. Ronsheim, M. Jeong, A. Grill, and H.-S. P. Wong, *Symposium on VLSI Technology Digest of Technical Papers*, pp.59-60, 2001.
- [4] M. L. Lee, Eugene A. Fitzgerald, Mayank T. Bulsara, Matthew T. Currie, and Anthony Lochtefeld, *J. Appl. Phys. Vol. 97, 011101*, 2005
- [5] Scott E. Thompson, Robert S. Chau, Tahir Ghani, Kaizad Mistry, Sunit Tyagi, and Mark T. Bohr, *IEEE T. Semiconduct. M. Vol. 18, No. 1*, pp. 26, 2005
- [6] X. Huang, W.-C. Lee, C. Kuo, D. Hisamoto, L. Chang, J. Kedzierski, E. Anderson, H. Takeuchi, Y.-K. Choi, K. Asano, V. Subramanian, T.-J. King, J. Bokor, and C. Hu, "Sub 50-nm FinFET: PMOS," *IEEE T. Electron Dev. Vol. 48, No. 5*, pp. 880, 2001
- [7] S. Takagia, T. Maeda, N. Taoka, M. Nishizawa, Y. Morita, K. Ikeda, Y. Yamashita, M. Nishikawa, H. Kumagai, R. Nakane, S. Sugahara and N. Sugiyama, *Microelectron. Eng. Vol. 84*, pp.2314, 2007.
- [8] Hiroshi Matsubara, Takashi Sasada, Mitsuru Takenaka, and Shinichi Takagi, *Appl. Phys. Lett. Vol. 93, 032104*, 2008.
- [9] K. Prabhakaran, F. Maeda, Y. Watanabe, and T. Ogino, *Appl. Phys. Lett. Vol. 76*, 2244, 2000.
- [10] J. Oh and J. C. Campbell, *J. Electron. Mater. Vol. 33*, pp.364, 2004.
- [11] S. Van Elshocht, B. Brijs, M. Caymax, T. Conard, T. Chiarella, S. De Gendt, B. De Jaeger, S. Kubicek, M. Meuris, B. Onsia, O. Richard, I. Teerlinck, J. Van

- Steenbergen, C. Zhao, and M. Heyns, *Appl. Phys. Lett. Vol. 85*, 3824, 2004.
- [12] N. Lu, W. Bai, A. Ramirez, C. Mouli, A. Ritenour, M. L. Lee, and D. Antoniadis, *Appl. Phys. Lett. Vol. 87*, 051922, 2005.
- [13] Q. Zhang, N. Wu, D. M. Y. Lai, Y. Nikolai, L. K. Bera and C. Zhu, *J. Electrochem. Soc. Vol. 153*, G207, 2006.
- [14] Y. Kamata, *Mater. Today, Vol. 11*, pp.30, 2008.
- [15] K. Zosel, and *Angew. Chem. Int. Ed. Engl, Vol. 17*, pp.702, 1978.
- [16] P. M. F. Paul, and W. S. Wise, *Mills&Boon, Ltd*, 1971.
- [17] C. W. Wang, R. T. Chang, W. K. Lin, R. D. Lin, M. T. Liang, J. F. Yang, and J. B. Wang, *J. Electrochem. Soc. Vol. 146*, pp.3485, 1999.
- [18] P. T. Liu, C. T. Tsai, T. C. Chang, K. T. Kim, P. L. Chang, C. M. Chen, and H. F. Cheng, *Electrochem. Solid- state Lett. Vol. 9*, G124, 2006.
- [19] P. T. Liu, C. T. Tsai, T. C. Chang, K. T. Kin, P. L. Chang, C. M. Chen, Y. C. Chen, *IEEE Trans. on Nanotech. Vol. 6*, pp.29, 2007.
- [20] P. T. Liu, C. T. Tsai, and P. Y. Yang, *Appl. Phys. Lett. Vol. 90*, 223101, 2007.
- [21] Y. Kamata, Y. Kamimuta, T. Ino and A. Nishiyama, *Jpn. J. Appl. Phys. Vol. 44*, No. 4B, pp. 2323, 2005
- [22] D. Tsoutsou, G. Apostolopoulos , S. Galata , P. Tsipas , A. Sotiropoulos , G. Mavrou , A. Dimoulas and Y. Panayiotatos , *Microelectron. Eng. Vol. 86*, pp. 1626, 2009
- [23] X. Zou, J. P. Xu, C. X. Li and P. T. Lai, *Appl. Phys. Lett. Vol. 90*, 163502, 2007.
- [24] J. F. Brennecke and C. A. Eckert, "Phase equilibria for supercritical fluid process design", *AIChE Journal*, **35**, p. 1049, 1989.
- [25] J. B. Rubin, L. B. Davenhall, C. M. V. Taylor, L. D. Sivils, T. Pierce, and K. Tiefert, "CO₂-Based Supercritical Fluids as Replacements for Photoresist-Stripping Solvents", *International LANL*, 1998.

- [26] L. B. Rothman, R. J. Robey, M. K. Ali, and D. J. Mount, "Supercritical fluid processes for semiconductor device fabrication", *IEEE/SEMI Advanced Semiconductor manufacturing Conference*, p. 372, 2002.
- [27] W. H. Mullee, M. A. Biberger, and P. E. Schilling, *United States Patent*, Patent 6500605 B1, 2002.
- [28] M. A. Biberger, P. Schilling, D. Frye, and M. E. Mills, "Photoresist and Photoresist Residue Removal with Supercritical CO₂—A Novel Approach to Cleaning Wafers", *SEMICONDUCTOR FABTECH 12TH*, p. 239.
- [29] S. Gangopadhyay, J.A. Lubguban, B. Lahlouh, G. Sivaraman, K. Biswasa, T. Rajagopalan, N. Biswas, H. C. Kim, W. Volksen and R. D. Miller, "Supercritical CO₂ Treatments for Semiconductor Applications", *Proc. Mat. Res. Soc. Symp.*, p. 812, 2004.
- [30] K. Prabhakaran and T. Ogino, "Oxidation of Ge(100) and Ge(111) surfaces: an UPS and XPS study," *Surface Science*, vol. 325, pp. 263-271, 1995.
- [31] R. van Eldik and F.-G. Klärner, *High Pressure Chemistry: Synthetic, Mechanistic, and Supercritical Applications*. Weinheim: Wiley-VCH, 2002.
- [32] K.-N. Choo, S.-I. Pyun, and Y.-S. Kim, "Oxidation and hydrogen uptake of Zr based Nb alloys at 400°C under 10 MPa H₂O steam atmosphere," *J. Nucl. Mater.*, vol. 226, pp. 9-14, 1995.
- [33] W. L. Hansen, E. E. Haller, and P. N. Luke, "Hydrogen Concentration and Distribution in High-Purity Germanium Crystals," *IEEE Trans. Nucl. Sci.*, vol. 29, pp. 738-744, 1982.
- [34] K. Kita, S. Suzuki, H. Nomura, T. Takahashi, T. Nishimura, and A. Toriumi, "Direct Evidence of GeO Volatilization from GeO₂/Ge and Impact of Its Suppression on GeO₂/Ge Metal–Insulator–Semiconductor Characteristics," *Jpn. J. Appl. Phys.*, vol. 47, pp. 2349-2353, 2008.